Agricultural Water Management 247 (2021) 106725

Contents lists available at ScienceDirect

Agricultural Water Management

journal homepage: www.elsevier.com/locate/agwat

Energy balance and irrigation performance assessments in lemon orchards by applying the SAFER algorithm to Landsat 8 images

Antônio Teixeira [a,*], Janice Leivas [b], Tiago Struiving [c], João Reis [d], Fúlvio Simão [d]

[a] Water Resources Program (PRORH) from Federal University of Sergipe (UFS), Brazil
[b] Embrapa Territory, Brazil
[c] Lemon Producers Association (ASLIM), Brazil
[d] Agricultural Research Corporation of Minas Gerais (EPAMIG), Brazil

ARTICLE INFO

Handling Editor: Dr. B.E. Clothier

Keywords:
Evapotranspiration
Crop coefficient
Irrigation systems
Citrus limon L

ABSTRACT

In the semiarid conditions of the São Francisco River Basin, Brazil, irrigated fruit crops are replacing natural vegetation, being lemon highlighted by incentives for the national and international markets. This paper aimed to support the rational water management of lemon orchards under different irrigation systems under these conditions. We present a methodology based on the use of the visible and near infrared images from Landsat 8 (L8) satellite together with weather and actual yield data (Y_a), to assess the energy balance components and irrigation performance indicators (IPI) by applying the SAFER (Simple Algorithm for Evapotranspiration Retrieving) in six commercial farms under different irrigation systems inside the basin in the northern Minas Gerais state, Southeast Brazil. The ET rates averaged 2.7 mm d^{-1}, 2.9 mm d^{-1}, and 3.7 mm d^{-1}, for drip, micro sprinkler, and pivot irrigated orchards, respectively. The evaporative fraction (latent heat flux by the available energy) reached above 1.00 for localized irrigation (drip and micro sprinkler), and 1.30 for pivots, during the lemon phenological stages from fruit growth to harvest peaks. Pivot irrigation systems were not recommended under the semi-arid conditions, due to large water direct evaporated from the soil and air close to the surface. For drip and micro sprinkler irrigated orchards, crop coefficient curves were modeled based on the accumulated degree-days (DD_{ac}) to estimate lemon crop water requirements. Drip irrigated orchards presented better water productivity levels being recommended together with deficit irrigation strategies which could allow good lemon yields with saving water savings. The most important findings of the current research are that the SAFER algorithm can be applied to estimate crop ET with satellite images without the thermal bands which together with modelled Y_a data, irrigation assessments can be carried out at high spatial resolution following the principles of precision agriculture. For replication of the methods in other regions, simple calibrations of the modelling equations can be performed to infer the specific environmental conditions.

1. Introduction

Citrus is a high water-requiring evergreen perennial crop, mainly growing in the tropics (Panigrahi and Srivastava, 2016). Among the lemon (*Citrus limon* L.) producing countries around the world, Brazil stands out with the highest yields, with Minas Gerais state (MG) ranking in the second national position (Gonçalves et al., 2020). In the northern MG, commercial lemon orchards have been growing under the semi-arid conditions of the São Francisco river basin, because of the Jaíba irrigation scheme at the vicinities of the River, which was built to promote sustainable regional development, based on irrigated agriculture, mainly fruit crops. Irrigation scheme here refers to the total irrigation complex, irrigation systems, the irrigated land, buildings, and roads (Bos et al., 2015). Under these circumstances, crop water consumption and crop water requirements must be optimized inside the scheme, designing an optimal irrigation strategy to maximize yield while promoting water savings (Jamshidi et al., 2020).

The Jaíba irrigation scheme encompasses the municipalities of Jaíba and Matias Cardoso, which together account for 70% of the whole lemon production in MG, with large participation in the international market (Gonçalves et al., 2020). However, caution must be taken regarding the rapid replacement of the natural vegetation by irrigated orchards in the

* Corresponding author.
E-mail addresses: heriberto@pq.cnpq.br, heribert@globomail.com (A. Teixeira), janice.leivas@embrapa.br (J. Leivas), stuiving@gmail.com (T. Struiving), jbrsreis.fulvio@epamig.br (J. Reis).

https://doi.org/10.1016/j.agwat.2020.106725
Received 3 June 2020; Received in revised form 23 December 2020; Accepted 23 December 2020
Available online 12 January 2021

Brazilian semiarid region due to alterations on the energy and water balance components. The main impacts caused by the land-use changes on the environment are the large water withdrawals from the São Francisco River, reducing its flow to the ocean, and the pollution caused by the agricultural drainage, increasing water competitions among different water users (Teixeira et al., 2018, 2020).

Good efficiencies of irrigation systems are extremely important to reduce actual evapotranspiration (ET) while preserving crop yield (Hatfield and Dold, 2019), i.e., increasing water productivity for a sustainable agriculture, which here is considered as the ratio of actual yield (Y_a) to ET (WP_{ET}) (Nyoley et al., 2019). According to Consoli et al. (2017), maintaining high WP_{ET} levels, is an important goal, when water resources are limited, but also in view of mitigating the negative environmental impacts of irrigation, such as threats to groundwater caused by excessive leaching of agrochemicals (Dahan et al., 2014). Most lemon orchards in the Brazilian semi-arid region are drip and micro sprinkler irrigated. These localized irrigation systems are considered the most efficient water distribution systems and allows increasing citrus WP_{ET} if coupled with effective water-saving irrigation management strategies (Rallo et al., 2017).

To determine ET in sparse irrigated orchards, one suitable way is trough quantifications of the radiation and energy balance components (Consoli and Papa, 2013). After considering all the radiation balance components, the net radiation (R_n) is the difference between incoming and outgoing radiation of both short and long wavelengths. An accurate determination of R_n is critical for the assessment of R_n-dependent processes, such as ET (Zheng et al., 2016; Ramírez-Cuesta et al., 2018). R_n is partitioned into latent (λE), sensible (H), and soil (G) heat fluxes, but at daily timescales G may be neglected for irrigation management (Consoli and Papa, 2013). In scenarios of climate and land use changes, λE is important, because it represents the energy for ET, which is the main use of the water resources by agriculture, when the crops are under good water status. On the other hand, the magnitude of H can indicate surface warming or cooling effects (Bhattarai et al., 2017a; Teixeira et al., 2017a).

An effective water supply through precise irrigation, is one of the pathways to sustain agriculture with high WP_{ET} levels (Panigrahi and Srivastava, 2016; Jamshidi et al., 2020). According to Nawaz et al (2020), the energy partition has substantial effects on fruit growth and development phases as well as physical characteristics of citrus, being ET the major consumptive use of irrigation water and precipitation in semi-arid regions, and any attempt to improve WP_{ET} must be based on reliable ET estimates (Consoli and Vanella, 2014). A well scheduled and dosed irrigation regime is essential for matching crop water requirements, which in turn require ET estimations (Gu et al., 2017; Gong et al., 2019). A practical way to estimate ET is through the K_c approach, and for this purpose, it is important to make distinctions between the concepts of reference (ET_0), actual (ET), and potential (ET_p) evapotranspiration, adopted in the current paper. ET_0 is the reference evapotranspiration calculated with weather data, while ET is the water flux involving all environmental conditions, and ET_p is considered to happen when the crop is under optimum root-zone moisture conditions (Allen et al., 1998). ET may deviate from ET_p due to water stress, and these deviations will affect the yield and quality of lemons.

In well-irrigated orchards, i.e, without water stress, the values of the root-zone moisture index ET/ET_0 may be considered as K_c being ET replaced by ET_p ($K_c = ET_p/ET_0$) (Consoli and Papa, 2013; Mateos et al., 2013; Consoli and Vanella, 2014; Longo-Minnolo et al., 2020). K_c may be partitioned into the transpiration (K_{cb}) and evaporation (K_e) components (Longo-Minnolo et al., 2020) and several studies have assessed crop water requirements from these single (K_c) and dual (K_{cb} and K_e) approaches (Jamshidi et al, 2020). On the other hand, under non--optimum root-zone moisture situations, low ET/ET_0 values characterize crop water stress (Lu et al., 2011). While K_c multiplied by ET_0, one estimate ET_p (Ramírez-Cuesta et al., 2019a), when including a stress coefficient (K_s), it is possible to retrieve ET under water limited conditions (Rallo et al., 2017; Longo-Minnolo et al., 2020; Jamshidi et al., 2020).

Single K_c values for improving irrigation management have been determined through field measurements in Brazil (Teixeira et al., 2008a; Marin et al., 2019); however, remote sensing from satellite images is another powerful way for K_c modelling that has also been used in different Brazilian agroecosystems, through vegetation indices (Silva et al., 2018; Teixeira et al., 2019). The upper limit of the ET/ET_0 pixel values during a growing season or a year may be used to fit a representative K_c curve, for estimation crop water requirements, when aiming to irrigation performance assessments (Teixeira et al., 2014a, 2014b). However, the adoption of deficit irrigation strategies by adding K_s values, is desirable for saving water while ensuring food yield levels, mainly in scenarios of water scarcity conditions, what have been done for orange orchards growing in semi-arid regions (Germaná and Sardo, 2004; Panigrahi and Srivastava, 2016; García Tejero et al., 2010, 2019; Jamshidi et al., 2020; Longo-Minnolo et al., 2020).

Although energy and water balance field measurements have been done by different methods in some Brazilian agroecosystems (Teixeira et al., 2008a, 2008b; Cabral et al., 2015; Marin et al., 2019), few efforts have been carried out in irrigated lemon orchards bring site-specific results (Junior et al., 2008), not suitable for irrigation performance assessments at commercial farm levels (Zheng et al., 2016; Bhattarai et al., 2017b; Nyoley et al., 2019), especially under semi-arid conditions with advective heat advections from the drier areas at the vicinities of the irrigated orchards (Consoli and Vanella, 2014). Besides variations of these balances with the weather, they will also depend on the root-zone moisture levels, which in turn are related to irrigation water management.

Due to limitations of field measurements at the irrigation scheme scale, up-scaling tools based on remote sensing from satellite images are important for crop water management decisions (Kamble et al., 2013; Zheng et al., 2016; Wagle et al., 2016; Bhattarai et al., 2017b, Ramírez-Cuesta et al., 2018; Tazekrit et al., 2018; Holtzman et al. 2018; Nyoley et al., 2019; Teixeira et al., 2019; Santos et al., 2020; Mhawej et al., 2020a, 2020b), which, from the knowledge of the authors of the current paper, have not yet been performed on farm scales for lemon orchards covering different irrigation systems. A generalized use of these tools requires a deep knowledge of biophysical variables and their relations with remote sensing parameters (Cancela et al., 2019). Remote sensing algorithms to quantify the energy and water balance components were previously developed, presenting advantages and shortcomings, for example, SEBAL - Surface Energy Balance Algorithm for Land (Bastiaansssen et al., 1998), S-SEBI - Simplified Surface Energy Balance Index (Roerink et al., 2000); SEBS - Surface Energy Balance System (Su, 2002), and the ET-Watch (Wu et al., 2008). These algorithms can be used to estimate ET and crop water requirements at farm level (Mhawej et al., 2020a, 2020b).

For operational purposes, the Penman-Monteith (PM) equation has been suggested by applying remotely sensed vegetation indices (VI), together with agrometeorological data (Cleugh et al., 2007; Nagler et al., 2013; Consoli and Vanella, 2014). The use of these PM-based methods has been suggested due to their simplicities and operationalities, while maintaining the physical basis (Consoli et al., 2016; Olivera-Guerra et al., 2018). When together with weather interpolation processes these methods are suitable for applying to satellite of low temporal resolutions (Mateos et al., 2013), requiring few inputs including phenological stage, irrigation amounts, and standard weather data (Vanella et al., 2019). The PM equation is also applied in the METRIC - Mapping Evapotranspiration with High Resolution and Internalized Calibration algorithm (Allen et al., 2007), an improved version of the SEBAL algorithm, which allow to up scale the satellite overpass ET to longer timescale, by calculating ET_0 from hourly weather data.

SEBAL and METRIC are nowadays the most used algorithms for ET estimations, however, the difficulties for applications of their original versions, is the requirement of hot and cold pixels in a scene, which is difficulty during rainy conditions because the absence of zero λE for the

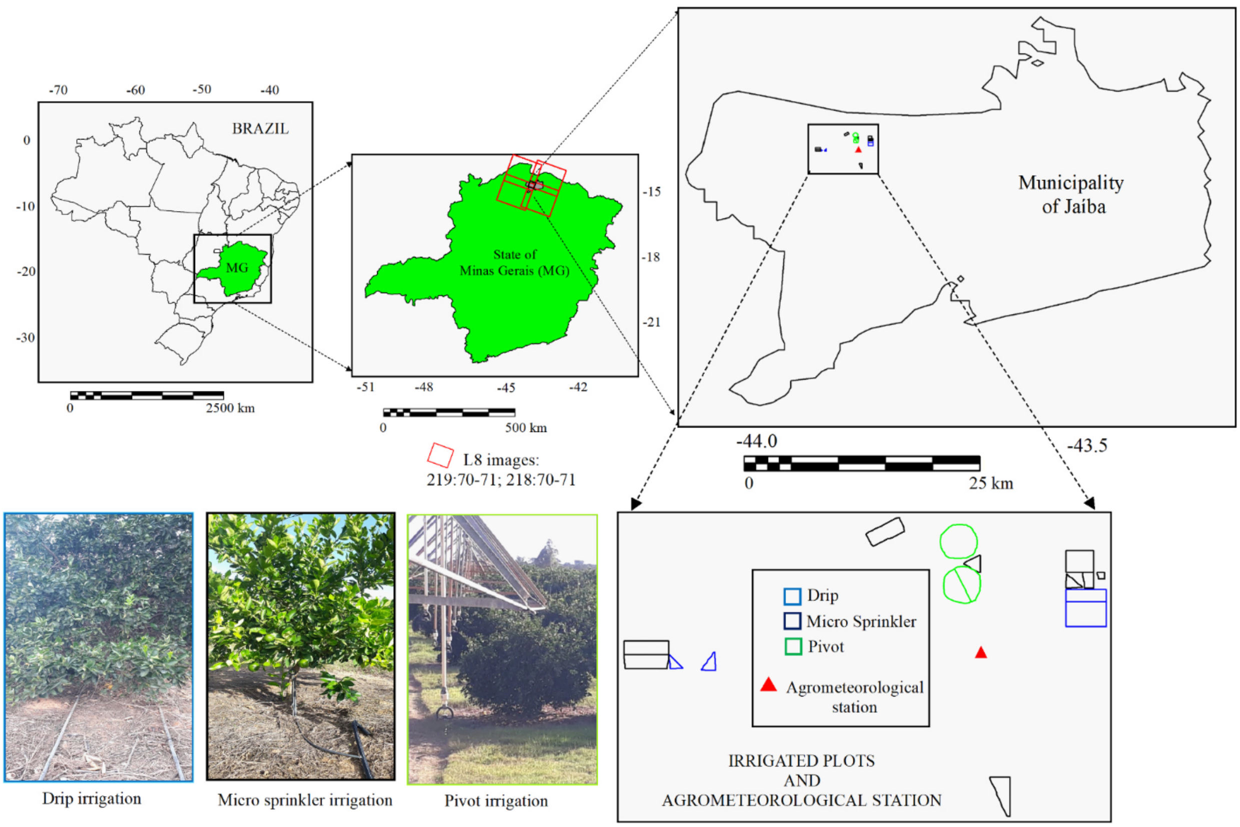

Fig. 1. Locations of the irrigated lemon orchards, in the municipality of Jaíba, semiarid region of the São Francisco river basin, northern Minas Gerais state (MG), Southeast Brazil, together with the agrometeorological station used. Highlights are given for the irrigation systems (drip, micro sprinkler, and pivot), and the orbital/pointer of the Landsat 8 images used.

required hot one. On the other hand, selecting these anchor pixels is labor intensive over large spatial areas or long time series if it is done manually (Lee and Kim, 2016). To overcome this difficult, this process has been solved by automating this selection eliminating the need for user-intervention (Bhattarai et al., 2017b; Jaafar and Ahmad, 2020). For instance, Mhawej et al. (2020a, 2020b) proposed some improvements in SEBAL by considering only agricultural areas, validating a dynamic calibration approach to retrieve ET, related to wind speed and air humidity conditions over water bodies.

By using time-series of Landsat images in Lebanon, Jaafar and Ahmad (2020) compared ET estimations from applications of the modified versions of METRIC and SEBAL, which have automated procedures to identify the hot and cold pixels. The authors concluded that the two models give comparable water use estimates at the seasonal and annual time steps. The modified version of SEBAL was also applied in South Korea to MODIS images for retrieving ET (Lee and Kim, 2016), but the low resolution of the thermal band (1000 km) brought the need of using temperature data from weather stations to fill gaps due clouds and/or snow and, according to the authors, errors in surface temperatures have great impacts on H estimations.

Aiming to subsidize water resources use, which include better agricultural crop management practices, the improved version of SEBAL was also used with MODIS images in a cultivated African catchment, Tanzania, by Nyoley et al. (2019), to estimate ET, and then derive WP_{ET} values by coupling Landsat 8 and Sentinel 2 images at a spatial resolution of 10 m. The authors reported satisfactory results when crossing with local information on crop yields, water allocation, and agricultural management practices in different agroecological zones within the catchment. Zheng et al. (2016) calibrated the original SEBAL empirical equations, coupling a radiation module on MODIS data in an arid land of Central Asia to better estimated ET, reporting improvements on the estimations of available energy (R_n – G) when comparing with the original equations in the SEBAL algorithm. However, although automation procedures reduce the bias in the output ET, these algorithms still require conditions for the anchor pixels (Jaafar and Ahmad, 2020). In addition, METRIC being based on a similar approach with SEBAL, requires high quality hourly weather data for ET calculations (Lee and Kim, 2016).

Satellite images for irrigation performance assessments in orchards has been used previously in an irrigation scheme in Northeast Brazil, by applying the SEBAL algorithm to NOAA images (Bastiaansssen et al., 2001). However, the spatial resolution of 1.1 km implies that land-cover in the pixels is a mixture of different surface types. According to Longo-Minnolo et al. (2020), the remote sensing results in citrus orchard

Table 1
Phenological stages for irrigated the lemon orchards, in the Jaíba irrigation scheme, semi-arid region of the São Francisco River basin, northern Minas Gerais state (MG), Southeast Brazil.

MONTH/ STAGE[1]	01	02	03	04	05	06	07	08	09	10	11	12
F			■	■				■	■			
FG				■	■	■			■	■	■	
HP	■	■				■	■	■			■	■

[1]F – Flowering; FG – Fruit Growth; HP – Harvest Peaks

Table 2
Lemon farms, rootstocks, cultivars, planting dates, spacings, areas, irrigation systems, and productivities (Prod) in 2015, in the Jaíba irrigation scheme in the semi-arid region of the São Francisco River basin, northern Minas Gerais state (MG), Southeast Brazil.

Farm[a]	Rootstock	Cultivar	Planting Date	Spacing (m)	Area (ha)	Irrigation System	Prod (t ha^{-1})
ES	Rangpur Lime	*IAC5*	03/2008	8.0 x 5.0	22.00	Micro	26.2
YA	Rangpur Lime	*IAC5*	01/2010	7.5 x 6.3	10.93	Micro	30.5
	Citrumelo	*Quebra Galho*	01/2010	7.5 x 5.0	23.87	Pivot	36.2
	Rangpur Lime	*IAC5*	01/2010	7.5 x 5.0	22.41	Pivot	27.7
SF	Rangpur Lime	*IAC5*	09/2009	7.0 x 6.0	21.66	Micro	37.5
	Rangpur Lime	*IAC5*	09/2009	7.0 x 6.0	20.89	Micro	30.5
	Rangpur Lime	*IAC5*	03/2010	7.0 x 6.0	3.06	Drip	16.2
	Rangpur Lime	*IAC5*	03/2010	7.0 x 6.0	3.87	Drip	14.3
SA	Rangpur Lime	*Quebra Galho*	08/2010	7.0 x 5.0	35.78	Drip	34.1
	Fly Dragon	*IAC5*	08/2010	6.0 x 3.0	18.15	Drip	40.1
MA	Fly Dragon	*IAC5*	01/2012	7.5 x 3.0	9.96	Micro	14.2
	Rangpur Lime	*Quebra Galho*	01/2010	7.0 x 5.0	5.48	Micro	24.8
	Rangpur Lime	*IAC5*	01/2007	7.0 x 5.0	13.24	Micro	35.9
TR	Rangpur Lime	*IAC5*	11/ 2009	7.0 x 5.0	17.85	Micro	21.2

[a] ES – Esperança; YA – Yamada; SF – Santa Fé; SA – Saara; MA – Marazul; and TR – Tropical

may be influenced by the pixel heterogeneity, containing vegetated and bare soil surfaces, highlighting the need of higher resolution images. Although SEBAL had been calibrated and validated with simultaneous field and Landsat satellite measurements, demonstrating a good performance in Brazilian semi-arid region of the São Francisco river basin (Teixeira et al., 2009a), the greatest difficulty for its application during the rainy season in this region is the absence of zero λE for the required hot pixel. Teixeira et al. (2009b) have reported that under these conditions, native *Caatinga* species can present λE rates even higher than those for irrigated orchards.

Considering the operationality of the PM equation for large-scale applications, the SAFER (Simple Algorithm for Evapotranspiration Retrieving) algorithm was developed by using simultaneous field and remote sensing measurements, for determining the energy and water balance components (Teixeira et al., 2008a, 2008b, Teixeira, 2010). To apply SAFER, it is not necessary selection of anchor pixels in the scene and it requires daily weather data. SAFER was previously called PM2, being after validated in a range of agroecosystems in Southeast Brazil (Coaguila et al., 2017; Silva et al., 2018; Santos et al., 2020; Rampazo et al., 2020). In addition, with its actual version, it is possible to estimate the energy and water balance components with and without the satellite thermal bands. In this last case only the visible and near infrared bands are used (Teixeira et al., 2019; Araujo et al., 2019; Silva et al., 2019; Teixeira et al., 2020), allowing analyses of irrigated areas at better spatial resolution with satellite images without the thermal spectrum. According to Consoli and Vanella (2014), the main advantage is that satellite imagery in the reflective bands are more readily available than the thermal band data, and generally at higher spatial resolution.

The objective of the current study was to test the application of latest version of the SAFER algorithm by using the visible and near infrared bands of the Landsat 8 images together with weather data at a 30-m spatial resolution, to retrieve the energy and water balance parameters in commercial lemon orchards, under drip, micro sprinkler, and pivot irrigation systems, for irrigation performance assessments, in the agricultural growing semi-arid region of the São Francisco river basin, in the northern Minas Gerais state, Southeast Brazil. The results would be important to generate criteria for improving lemon irrigation practices in this region, but the success of these local specific applications, may allow replication of the methods in other semi-arid environments around the world, probably requiring only simple adjustments in the regression coefficients of the modelling equations.

2. Materials and methods

2.1. Characteristics of the study area

Fig. 1 shows the locations of the lemon orchards, under different irrigation systems, together with the agrometeorological station, in the municipality of Jaíba, semiarid region of the São Francisco river basin, northern Minas Gerais state (MG), Southeast Brazil.

The study area has a central latitude and longitude of 15° 20' 14'' S and 43° 41' 09'' W, respectively, at a mean altitude of 475 m. This region has tropical dry and hot climate, with an average annual precipitation (P) is 860 mm yr^{-1}, although varying along the years and strongly irregularly distributed within a year, with 90% of rains concentrated in the first (January-April) and fourth (September-December) quarters of the year. The annual ET_0 is 1335 mm yr^{-1}, thus, accounting for P and ET_0, there is an annual climatological water deficit of 475 mm yr^{-1}. The thermal regime is characterized by high air temperatures (T_a), with an annual average of 24.0 °C and long-term monthly maximums from September to October, between 31.0 and 32.0 °C. The corresponding minimums are between 14 and 17 °C in June and July, respectively, during the winter solstice of the southern hemisphere (Lumbreras et al., 2014).

In the northern MG, the ecosystems under the semi-arid conditions of the São Francisco River basin, have distinct and typical vegetation, most corresponding to *Caatinga* species, but with a transition area with savanna (Costa et al., 2010). Inside the Jaíba irrigation scheme, agricultural crops are interspersed with these natural species, which are brown outside the rainy period, strongly contrasting with irrigated areas, but as soon as the rains start, they become moist and green. Due to the irrigation technologies at the banks of the São Francisco River, natural vegetation is rapidly being replaced by irrigated crops, mostly commercial orchards (Leivas et al., 2016).

2.2. Crop conditions

Table 1 presents the phenological stages of the studied irrigated lemon orchards, considered by the Lemon Producers Association (ASLIM), in the Jaíba irrigation scheme.

According to ASLIM, lemon harvests occur during the whole year, but with two harvest peaks (HP) – in June/August and in November/February, being the main concentration of fruits from December to February. In the middle of the year, HP periods coincide with Flowering (F) and Fruit Growth (FG) stages, from June to August. The crop has two F periods during the year but mixed with FG stages in the same irrigated parcel; however, the bloom intensity depends on the weather and root-zone moisture conditions. The cropped lemon clones are the locally called *Quebra Galho* and *IAC5*, grafted on the rootstocks Rangpur lime (*Citrus limonia*), Fly Dragon (*Poncirus trifoliata*), and Citrumelo (*Citrumelo Swingle*).

Table 2 shows the analyzed producing lemon farms, rootstocks, cultivars, planting dates, spacings, areas, irrigation systems, and productivities (Prod) in 2015.

According to Table 2, the analyses involved plant ages from 3 to 8 years. The spacings are from 6.0 to 8.0 m between lines and 3.0–6.3 m between plants, with an average height of 3 m, in areas of 60.9, 122 and 46.3 ha irrigated by drip, micro sprinkler, and pivot systems,

Table 3
Characteristics of the bands used from the Landsat 8 (L8) satellite in the study region during 2015.

Satellite	Spatial Resolution	Spectral Bands (μm)	Imaging Sweep	Temporal Resolution	Orbital/ Pointer
Landsat 8	30 m	B1: 0.43–0.45	185 Km	16 days	218/70
		B2: 0.45–0.51			
		B3: 0.53–0.59			
		B4: 0.64–0.69			218/71
		B5: 0.85–0.88			219/70
		B6: 1.57–1.65			
		B7: 2.11–2.29			

*Image acquisition days in terms of day of the year (DOY):
Orbital/Pointer 218/70 – DOY: 003, 067, 115, 147, 211, 275, 307
Orbital/Pointer 218/71 – DOY: 243, 019, 131, 163, 259, 291, 355
Orbital/Pointer 219/70 – DOY: 010, 090, 154, 170, 186, 202, 218, 250, 266, 282, 314, 330, 346

respectively. Prod ranged between 14.2 and 40.1 t ha^{-1}, with the lowest level occurring under micro sprinkler irrigation and the highest one under drip irrigation, but with the same cultivar (*IAC5*) and rootstock (Fly Dragon). In the pivot irrigated areas there were high Prod levels (above 25.0 t ha$-^{1}$), but these levels also happened in drip and micro sprinkler irrigated orchards. Differences on Prod values may be attributed to plant ages, densities, irrigation systems and irrigation schedule, as well as rootstock/cultivar combinations.

2.3. Energy and water balance modelling

2.3.1. Data set and modelling steps

One agrometeorological station (Lat. 15° 13’ 54’’ S, Long. 43° 58’ 04’’ W, Alt. 454 m) close to the studied commercial lemon farms (Fig. 1), was used, from which daily weather data covered different thermohydrological conditions, along the year 2015 were modelling inputs. Daily data on global solar radiation (R_G), air temperature (T_a), relative humidity (RH), and wind speed at 2 m height (u_2) were used for computing daily ET_0 by the PM method (Allen et al., 1998) together with remote sensing parameters from Landsat 8 (L8) images, surface albedo (α_0) and the Normalized Difference Vegetation Index (NDVI). The agrometeorological station is programmed to collect data at each minute and storage half-hour averages and then 24-hour mean values were considered for the SAFER application.

The L8 scenes used were from orbital/pointer 218/70, 218/71 and 219/70, overlapping the study area on the same date (see Fig. 1). Overlapping satellite crossings, gave the opportunity of 27 image acquisitions, and when there were cloud problems, α_0 and NDVI were successively interpolated, by averaging the pixel values between dates, and then weather data for these cloudy days were used, allowing the assessments of energy balance components and irrigation performance, covering all irrigated lemon orchard phenological stages shown in Table 1. According to Mateos et al. (2013), interpolated vegetation indices are subject to less uncertainty than interpolated ET values obtained on satellite overpass days.

Table 3 shows the characteristics of the L8 bands used:

Fig. 2 presents the modeling steps for the energy balance and irrigation performance assessments by applying the SAFER algorithm.

L8 bands from 1 to 7 (spatial resolution of 30 m) were used to calculate α_0 (b_1 to b_7), being b_4 and b_5 used for NDVI, whereas the surface

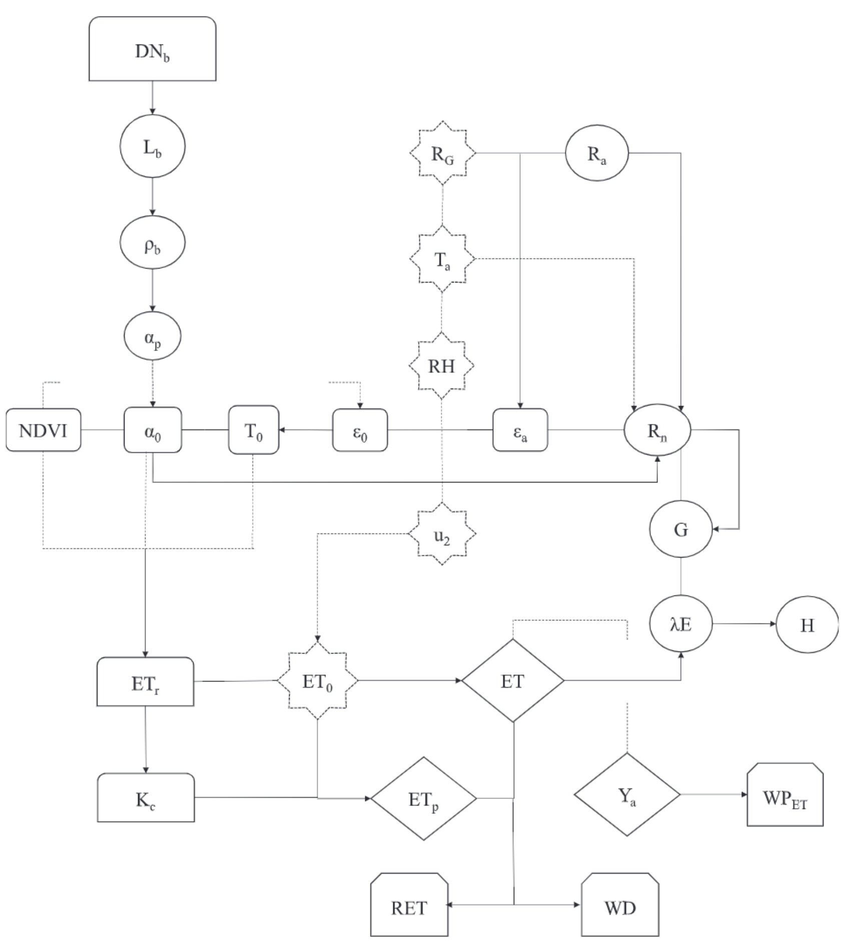

Fig. 2. Steps for the energy balance and irrigation performance assessments for lemon orchards, by applying the SAFER algorithm, in the semi-arid region of the São Francisco River basin, northern Minas Gerais state (MG), Southeast Brazil. Dashed polygonal shaped boxes are data from the agrometeorological station. Note: DN_b – Digital number from bands b1 to b7; L_b – Spectral radiances from bands b1 to b7; ρ_b – Reflectance from bands b1 to b7; α_p – Planetary albedo; α_0 – Surface albedo; NDVI – Normalized Difference Vegetation Index; T_0 – Surface temperature; ET_r – Ratio of the actual to reference evapotranspiration; R_G – Incident global solar radiation; T_a – Mean air temperature; RH – Relative Humidity; u_2 – Wind speed at 2 m height; ET_0 – Reference Evapotranspiration; K_c – Crop coefficient; R_a – Atmospheric radiation; R_n – Net radiation; ε_a – Atmospheric emissivity; ε_0 – Surface emissivity; ET – Actual Evapotranspiration; ET_p – Potential Evapotranspiration; RET – Relative Evapotranspiration; WD – Water Deficit; Y_a – Actual yield; WP_{ET} – Water Productivity based on ET; G – Soil heat flux; λE – Latent heat flux; H – Sensible heat flux.

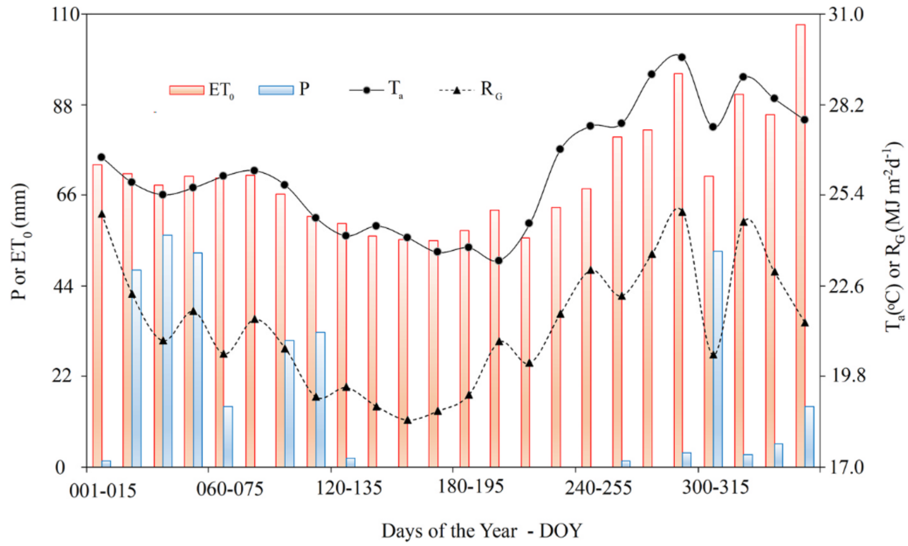

Fig. 3. Fortnightly values for totals of precipitation (P) and reference evapotranspiration (ET_0); and averages for daily global solar radiation (R_G) and air temperature (T_a) values, during 2015, according to the Days of the Year (DOY), in the Municipality of Jaíba, semi-arid region of São Francisco river basin, northern Minas Gerais (MG) state, Southeast Brazil.

temperature (T_0) was retrieved as residue in the radiation balance. This residual method has been successfully tested in distinct Brazilian agro-ecosystems (Teixeira et al., 2019, 2020; Araujo et al., 2019; Silva et al., 2019; Rampazo et al., 2020). The suitability of retrieving the energy and water balance components, without the satellite thermal bands, has been also demonstrated in other recent studies around the word (Castelli et al., 2018; Rozenstein et al., 2018; Vanino et al., 2018; Mokhtari et al., 2019; Longo-Minnolo et al., 2020). We opted for using the residual method to estimate T_0, to bring all pixel to suitable sizes (30 m) in relation to the lemon parcels. The use of the L8 thermal band retrieve T_0 from application of the Plank's low at satellite overpass time, while by its daily estimation from residue in the radiation balance we followed the physical principle of the Stefan Boltzmann equation for the emitted both atmospheric and surface radiation. Thus, in this way, it is possible to capture the water stress effects without the need of the thermal portion of the electromagnetic spectrum (Consoli and Vanella, 2014).

All the regression coefficients for SAFER application, described in Fig. 2 were previously determined and statistically analyzed against field measurements in semi-arid region of the São Francisco River basin, Brazil. In addition, acquiring T_0 as residue in the radiation balance gives mutual compensation, reducing possible errors in this model input parameter, as in the upward and downward long-wave fluxes, they are self-canceling. The algorithm was elaborated and validated with Landsat images (Teixeira, 2010) when it was called PM2. Later, it was also calibrated and validated in several agroecosystems under semiarid conditions of the basin (Araujo et al., 2019; Silva et al., 2019; Teixeira et al., 2020).

Field data used for the SAFER elaboration involved irrigated crops and natural vegetation (*Caatinga*) from 2001 to 2007, being described in detail in Teixeira et al. (2008b). Table grapes were micro sprinkler irrigated and conducted by an overhead trellis system, wine grapes were drip irrigated and conducted by a vertical trellis system, and mango orchard were micro sprinkler irrigated. The experimental period for *Caatinga* involved different species and rainfall conditions above and below the local long-term value. In addition, ET_r values under optimum root-zone moisture conditions in the current lemon study were checked with the crop coefficient (K_c) approach (Allen et al., 1998) from literature. Thus, with previous calibrations and validations, together with assumptions for the Brazilian semi-arid environments, one can expect sufficient accuracy for evaluations of the lemon energy balance and irrigation performance assessments among different irrigation systems under the study region conditions, being not strictly necessary new expensive validations with field data.

2.3.2. *Coupling remote sensing and agrometeorological data*

Following Fig. 2, the spectral radiances (L_b) from bands (b) 1–7, were computed from their Digital Numbers (DN_b):

$$L_b = a + bDN_b \tag{1}$$

where L_b is in W m^{-2} sr^{-1} μm^{-1}, and a and b are regression coefficients given in the metadata file (Vanhellemont and Ruddick, 2014).

The reflectance for each Landsat satellite band (ρ_b) was calculated by using the general equation:

$$\rho_b = \frac{L_b \pi d^2}{R_{a_b} \cos\varphi} \tag{2}$$

where d is the relative earth-sun distance; R_{a_b} is the mean solar irradiance at the top of the atmospheric irradiance for each band (W m^{-2} μm^{-1}), and φ the solar zenith angle.

R_{a_b} for each of the bands 1–7 of the L8 sensor was calculated according to the Planck's low, integrating the radiation over the wavelength intervals and considering its fraction over the solar spectrum, assuming the sun as a blackbody. The broadband planetary albedo (α_p) was then computed as the total sum of the ρ_b values, according to the weights for each band (w_b) (Teixeira et al., 2017b):

$$\alpha_p = \sum_{b_1}^{b_7} w_b \rho_b \tag{3}$$

For estimating α_0, atmospheric corrections were applied to the α_p values through regressions from previous field measurements and Landsat estimations of incident and reflected solar radiation, involving irrigated crops and natural vegetation under different weather conditions in the Brazilian semi-arid region (Teixeira et al., 2008b; Teixeira, 2010).

NDVI was calculated from the ρ_4 and ρ_5 pixel values:

$$NDVI = \frac{\rho_5 - \rho_4}{\rho_5 + \rho_4} \tag{4}$$

The atmospheric radiation (R_a) (W m^{-2}) was calculated by the Stefan-Boltzmann law (Ramírez-Cuesta et al., 2018):

$$R_a = \sigma \varepsilon_a T_a^4 \tag{5}$$

where σ is the Stefan-Boltzmann constant (5.67 x 10^{-8} W m^{-2} K^{-4}); T_a (K) was measured at the agrometeorological station, and ε_a is the atmospheric emissivity.

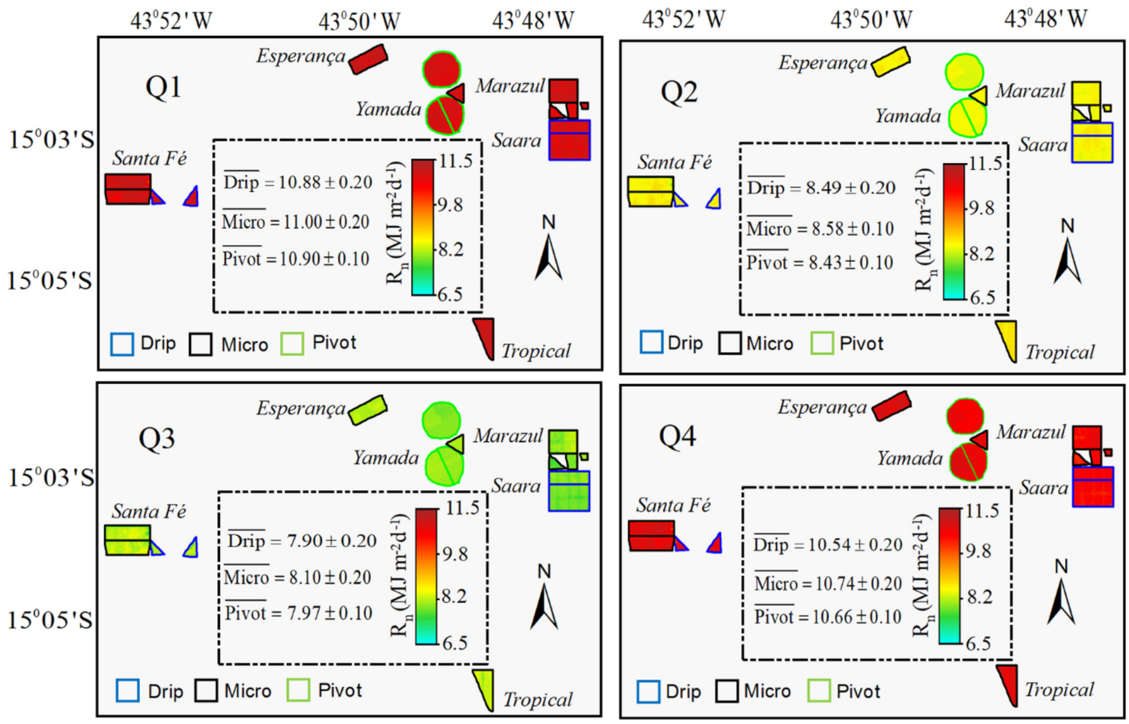

Fig. 4. Spatial distribution, averages, and standard deviations (SD), for the net radiation (R_n) quarterly values. Blue, black, and green contour lines represent lemon orchards irrigated by drip, micro sprinklers, and pivot irrigation systems, respectively, inside the commercial farms descried in Table 2. Q1– First quarter (January to March); Q2 – Second quarter (April to June); Q3 – Third quarter (July to September); Q4 – Fourth quarter (October to December). (For interpretation of the references to colour in this figure legend, the reader is referred to the web version of this article.)

Table 4
Average quarterly values and standard deviations (SD) for net radiation (R_n), in drip, micro sprinkler, and pivot irrigated lemon orchards of each studied commercial farm, in the semi-arid region of São Francisco river basin, northern Minas Gerais state (MG), Southeast Brazil.

Farm/Irrigation system	Net radiation - R_n (MJ m^{-2} d^{-1})				
[a]ES	[b]Q1	Q2	Q3	Q4	Year
Micro Sprinkler	11.05 ± 0.08a	8.58 ± 0.07b	8.12 ± 0.07a	10.87 ± 0.10b	9.66 ± 0.07
YA					
Micro Sprinkler	10.92 ± 0.07a	8.56 ± 0.05a	8.07 ± 0.05a	10.72 ± 0.07a	9.57 ± 0.06
Pivot	10.90 ± 0.08a	8.43 ± 0.08a	7.97 ± 0.08a	10.66 ± 0.12a	9.49 ± 0.08
SF					
Drip	10.86 ± 0.24a	8.45 ± 0.23a	7.96 ± 0.24a	10.60 ± 0.22a	9.47 ± 0.23
Micro Sprinkler	10.94 ± 0.19a	8.55 ± 0.19a	8.13 ± 0.22b	10.75 ± 0.25b	9.59 ± 0.20
SA					
Drip	10.90 ± 0.10a	8.52 ± 0.12a	7.84 ± 0.11a	10.47 ± 0.10a	9.43 ± 0.10
MA					
Micro Sprinkler	10.96 ± 0.12a	8.50 ± 0.10a	7.94 ± 0.17a	10.51 ± 0.17a	9.48 ± 0.13
TR					
Micro Sprinkler	11.11 ± 0.08b	8.72 ± 0.08b	8.23 ± 0.09b	10.83 ± 0.12b	9.72 ± 0.09

[a] ES – Esperança; YA – Yamada; SF – Santa Fé; SA – Saara; MA – Marazul; and TR – Tropical

[b] Q1– First quarter (January to March); Q2 – Second quarter (April to June); Q3 – Third quarter (July to September); Q4 – Fourth quarter (October to December). R_n rates with the same letter in each column indicate no significant differences from each other at 5% (pairwise comparisons using the Tuckey HSD post-hoc test performed for each quarter).

The daily values of R_n (W m^{-2}) were estimated by applying the Slob equation:

$$R_n = (1 - \alpha_0)R_G - a_L\tau_{sw} \quad (6)$$

with the regression coefficient a_L estimated through its relationship with T_a (Teixeira et al., 2008b).

The ε_a term from Eq. (5) was computed as a function of the shortwave atmospheric transmissivity ($\tau_{sw} = R_G/R_a$):

$$\varepsilon_a = a_A(\ln \tau_{sw})^{b_A} \quad (7)$$

with a_A and b_A being the regression coefficients. For the Brazilian semi-arid conditions, they are $a_A = 0.94$ and $b_A = 0.10$, resulted from field measurements or estimations of R_a, T_a and τ_{sw} (Teixeira et al., 2008b).

The surface emissivity (ε_0) was estimated according to Santos et al. (2020):

$$\varepsilon_0 = a_0 \ln(NDVI) + b_0 \quad (8)$$

with a_0 and b_0 being the regression coefficients. For the Brazilian semi-arid conditions, they are $a_0 = 0.06$ and $a_0 = 1.00$, resulted from field measurements of emitted surface radiation and T_0, together with remote sensing calculations of NDVI (Teixeira et al., 2008b; Teixeira, 2010).

By the residual method, T_0 was estimated applying the Stefan-Boltzmann equation applied to the emitted long-wave radiations (Ramírez-Cuesta et al., 2018):

Table 5
Average quarterly values for the net radiation (R_n) to global solar radiation (R_G) ratios, in drip, micro sprinkler, and pivot irrigated lemon orchards, in the semi-arid region of the São Francisco river basin, northern Minas Gerais state (MG), Southeast Brazil.

Quarter/Irrigation System	Q1[a]	Q2	Q3	Q4	Year
Drip	0.49	0.44	0.45	0.48	0.47
Micro Sprinkler	0.50	0.44	0.46	0.49	0.47
Pivot	0.50	0.43	0.46	0.48	0.47

[a] Q1– First quarter (January-March); Q2 – Second quarter (April-June); Q3 – Third quarter (July-September); Q4 – Fourth quarter (October-December).

$$T_0 = \sqrt[4]{\frac{R_G(1-\alpha_0) + \sigma\varepsilon_a T_a{}^4 - R_n}{\sigma\varepsilon_0}} \quad (9)$$

The evapotranspiration ratio, ET_r, i.e. the ratio of the actual (ET) to reference (ET_0) evapotranspiration, was estimated as (Teixeira, 2010):

$$ET_r = \exp\left[a_{sf} + b_{sf}\left(\frac{T_0}{\alpha_0 NDVI}\right)\right] \quad (10)$$

where a_{sf} and b_{sf} are regression coefficients, being respectively 1.8 and −0.008 for the semi-arid conditions of the São Francisco River basin, Brazil, resulted from simultaneous field and remote sensing measurements of ET and ET_0, and α_0, T_0 and NDVI, respectively (Teixeira et al., 2008b; Teixeira, 2010).

The daily ET_0 values were then multiplied by satellite overpass ET_r pixel values, giving the large-scale daily ET values, which in turn were transformed into energy units, resulting in the λE daily rates.

G was considered as a fraction of R_n and H estimated by residue in the energy balance equation (Teixeira et al., 2017b):

$$\frac{G}{R_n} = a_G \exp(b_G \alpha_0) \quad (11)$$

$$H = R_n - \lambda E - G \quad (12)$$

where a_G and b_G are regression coefficients, being respectively 3.98 and −25.47 for the semi-arid conditions of the São Francisco River basin, resulted from simultaneous field measurements of G, R_n, and α_0 (Teixeira et al., 2008b; Teixeira, 2010).

For assessments of the root-zone moisture conditions, besides ET_r, the evaporative fraction (E_f) was also used:

$$E_f = \frac{\lambda E}{(R_n - G)} \quad (13)$$

The above equations were applied involving the whole Jaíba irrigation scheme, encompassing irrigated crops, natural vegetation, buildings, and roads (Fig. 1). Shapes of the lemon orchards areas under different irrigation systems were built from GPS control points, and the energy balance and irrigation performance assessments were carried out cutting the pixels inside these shaped areas. The central portions of the individual lemon parcels were considered avoiding edge-pixel contaminations, and the averages and standard deviation (SD) values resulted from around 475, 940, and 360 pixels, were taken for further analysis and comparisons among the drip, micro sprinkler, and pivot irrigated orchards (Longo-Minnolo et al., 2020).

For statistical analyses, we performed a pairwise comparison by applying the Tuckey honestly significant difference (HSD) post-hoc test for the energy balance components, to analyse their differences at 5% significance level, regarding the irrigation systems (drip, micro sprinkler, and pivot), and quarters of the year (Q1 - January to March; Q2 - April to June, Q3 - July to September, Q4 - October to December).

For lemon crop irrigation performance assessments, the key parameters are precipitation (P) and irrigation (I); soil moisture conditions; actual evapotranspiration (ET); as well as the crop water requirements, represented by the potential evapotranspiration (ET_p); and actual yield (Y_a). As we did not have reliable data on I, the assessments were

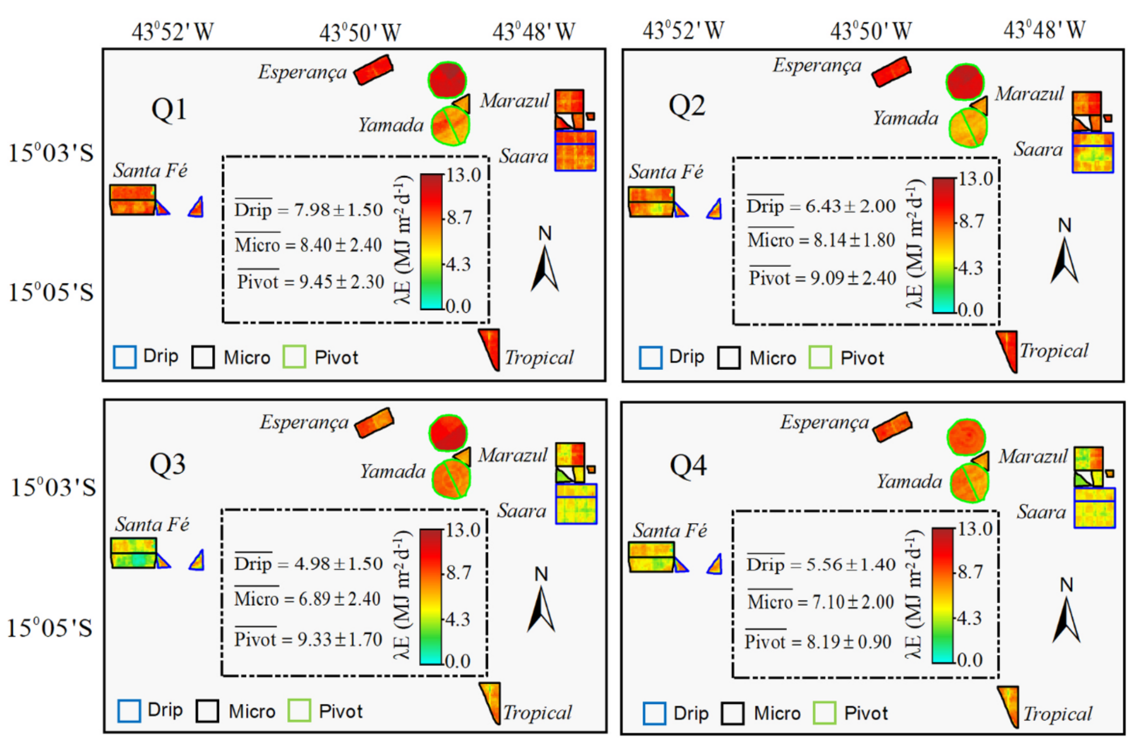

Fig. 5. Spatial distribution, averages, and standard deviations (SD), for the latent heat flux (λE) quarterly values. Blue, black, and green contour lines represent lemon orchards irrigated by drip, micro sprinklers, and pivot irrigation systems, respectively, inside the commercial farms from Table 2. Q1– First quarter (January to March); Q2 – Second quarter (April to June); Q3 – Third quarter (July to September); Q4 – Fourth quarter (October to December). (For interpretation of the references to colour in this figure legend, the reader is referred to the web version of this article.)

Table 6
Average quarterly values and standard deviations (SD) for latent heat flux (λE), in drip, micro sprinkler, and pivot irrigated lemon orchards of each studied commercial farm, in the semi-arid region of São Francisco river basin, northern Minas Gerais state (MG), Southeast Brazil.

Farm/Irrigation system	Latent heat flux - λE ($MJ\ m^{-2}\ d^{-1}$)				
[a]ES	[b]Q1	Q2	Q3	Q4	Year
Micro Sprinkler	8.88 ± 0.75b	9.04 ± 0.58b	8.24 ± 0.96b	8.70 ± 0.85b	8.72 ± 0.70
YA					
Micro Sprinkler	7.24 ± 0.55a	7.29 ± 0.67a	7.03 ± 0.56a	7.18 ± 0.66a	7.19 ± 0.58
Pivot	9.45 ± 2.33b	9.09 ± 2.44b	9.33 ± 1.65b	8.19 ± 0.90b	9.02 ± 1.71
SF					
Drip	7.73 ± 2.05a	6.56 ± 1.97a	4.85 ± 2.05a	5.94 ± 1.95a	6.27 ± 1.92
Micro Sprinkler	8.16 ± 1.46a	7.07 ± 1.79a	5.41 ± 1.75a	6.78 ± 1.55a	6.86 ± 1.52
SA					
Drip	8.22 ± 1.27a	6.29 ± 1.53a	5.11 ± 1.04a	5.38 ± 0.94a	6.25 ± 1.08
MA					
Micro Sprinkler	9.03 ± 0.88a	8.75 ± 0.91b	6.56 ± 2.01a	5.55 ± 1.90a	7.47 ± 1.31
TR					
Micro Sprinkler	8.68 ± 0.68b	8.55 ± 0.81b	7.19 ± 1.12a	7.31 ± 1.10b	7.93 ± 0.87

[a] ES – Esperança; YA – Yamada; SF – Santa Fé; SA – Saara; MA – Marazul; and TR – Tropical
[b] Q1– First quarter (January to March); Q2 – Second quarter (April to June); Q3 – Third quarter (July to September); Q4 – Fourth quarter (October to December). λE rates with the same letter in each column indicate no significant differences from each other at 5% (pairwise comparisons using the Tuckey HSD post-hoc test performed for each quarter).

Table 7
Average quarterly values for the latent heat flux (λE) to net radiation (R_n) ratios, in drip, micro sprinkler, and pivot irrigated lemon orchards, in the semi-arid region of the São Francisco river basin, northern Minas Gerais state (MG), Southeast Brazil.

Quarter/Irrigation System	Q1[a]	Q2	Q3	Q4	Year
Drip	0.73	0.76	0.63	0.54	0.66
Micro Sprinkler	0.76	0.95	0.85	0.66	0.79
Pivot	0.87	1.08	1.17	0.77	0.95

[a] Q1– First quarter (January-March); Q2 – Second quarter (April-June); Q3 – Third quarter (July-September); Q4 – Fourth quarter (October-December).

restricted to ET, soil moisture, ET_p, and Y_a data.

For K_c estimations in drip and micro sprinkler lemon irrigated areas, the average ET_r pixel values (Eq. (10)), summed by the upper limit of the SD values, were considered, allowing K_c modelling as a function of the accumulated degree-days (DD_{ac}), taking the basal temperature of 10 °C (Teixeira et al., 2014a).

$$K_{c_{Drip,Micro}} = a_{Drip,Micro}DD_{ac}^2 + b_{Drip,Micro}DD_{ac} + c_{Drip,Micro} \quad (14)$$

where $a_{Drip,Micro}$, $b_{Drip,Micro}$, and $c_{Drip,Micro}$ are regression coefficients

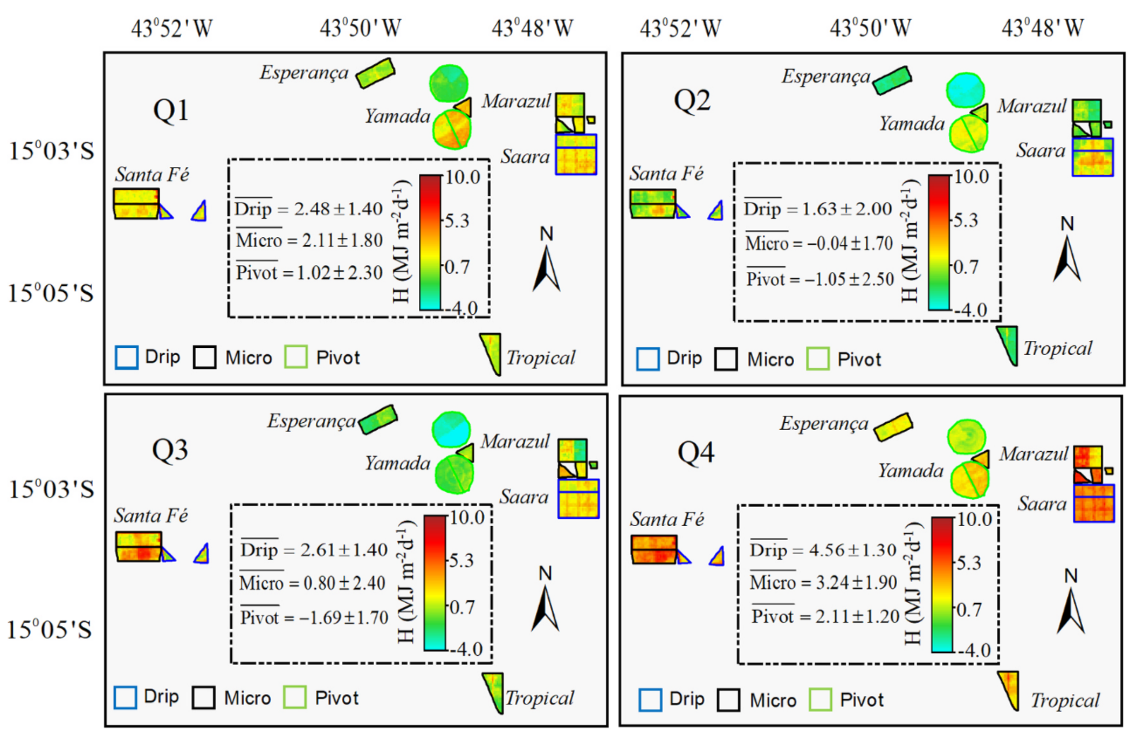

Fig. 6. Spatial distribution, averages, and standard deviations (SD), for the sensible heat flux (H) quarterly values. Blue, black, and green contour lines represent lemon orchards irrigated by drip, micro sprinklers, and pivot irrigation systems, respectively, inside the commercial farms from Table 2. Q1– First quarter (January to March); Q2 – Second quarter (April to June); Q3 – Third quarter (July to September); Q4 – Fourth quarter (October to December). (For interpretation of the references to colour in this figure legend, the reader is referred to the web version of this article.)

Table 8
Average quarterly values and standard deviations (SD) for sensible heat flux (H), in drip, micro sprinkler, and pivot irrigated lemon orchards of each studied commercial farm, in the semi-arid region of São Francisco river basin, northern Minas Gerais state (MG), Southeast Brazil.

Farm/Irrigation system	Sensible heat flux - H ($MJ\ m^{-2}\ d^{-1}$)				
[a]ES	[b]Q1	Q2	Q3	Q4	Year
Micro Sprinkler	1.66 ± 0.73a	-0.93 ± 0.57a	-0.53 ± 0.97a	1.73 ± 0.82a	0.48 ± 0.69
YA					
Micro Sprinkler	3.24 ± 0.52b	0.80 ± 0.65a	0.67 ± 0.54a	3.16 ± 0.66b	1.98 ± 0.56
Pivot	1.02 ± 2.32a	-1.05 ± 2.45b	-1.69 ± 1.73a	2.11 ± 1.16a	0.10 ± 1.83
SF					
Drip	2.71 ± 1.92b	1.48 ± 1.87b	2.76 ± 1.98b	4.32 ± 1.85b	2.82 ± 1.80
Micro Sprinkler	2.32 ± 1.37b	1.02 ± 1.73b	2.27 ± 1.74b	3.57 ± 1.39b	2.30 ± 1.44
SA					
Drip	2.25 ± 1.27b	1.77 ± 1.52b	2.45 ± 1.01b	4.79 ± 0.89b	2.81 ± 1.06
MA					
Micro Sprinkler	1.47 ± 0.87a	-0.69 ± 0.89a	1.05 ± 1.97a	4.65 ± 1.76b	1.62 ± 1.25
TR					
Micro Sprinkler	1.88 ± 0.65a	-0.42 ± 0.81a	0.53 ± 1.11a	3.10 ± 1.02a	1.27 ± 0.84

[a] ES – Esperança; YA – Yamada; SF – Santa Fé; SA – Saara; MA – Marazul; and TR – Tropical
[b] Q1– First quarter (January to March); Q2 – Second quarter (April to June); Q3 – Third quarter (July to September); Q4 – Fourth quarter (October to December). H rates with the same letter in each column indicate no significant differences from each other at 5% (pairwise comparisons using the Tuckey HSD post-hoc test performed for each quarter).

Table 9
Average quarterly values for the sensible heat flux (H) to net radiation (R_n) ratios, in drip, micro sprinkler, and pivot irrigated lemon orchards, in the semi-arid region of the São Francisco river basin, northern Minas Gerais state (MG), Southeast Brazil.

Quarter/Irrigation System	Q1[a]	Q2	Q3	Q4	Year
Drip	0.23	0.19	0.33	0.43	0.30
Micro Sprinkler	0.19	-0.01	0.10	0.30	0.16
Pivot	0.09	-0.12	-0.21	0.20	0.01

[a] Q1– First quarter (January-March); Q2 – Second quarter (April-June); Q3 – Third quarter (July-September); Q4 – Fourth quarter (October-December).

determined specifically for lemon orchards irrigated by drip (*subscript Drip*), and micro sprinkler (*subscript Micro*) systems.

The values of potential evapotranspiration (ET_p) were estimated according to Mateos et al. (2013):

$$ET_p = K_c ET_0 \tag{16}$$

Thus, the following irrigation performance indicators were considered (Bastiaansssen et al., 2001; Bos et al., 2015; Teixeira et al., 2014a; Fernández et al., 2019; Jamshidi et al, 2020):

$$RET = \frac{ET}{ET_p} \tag{17}$$

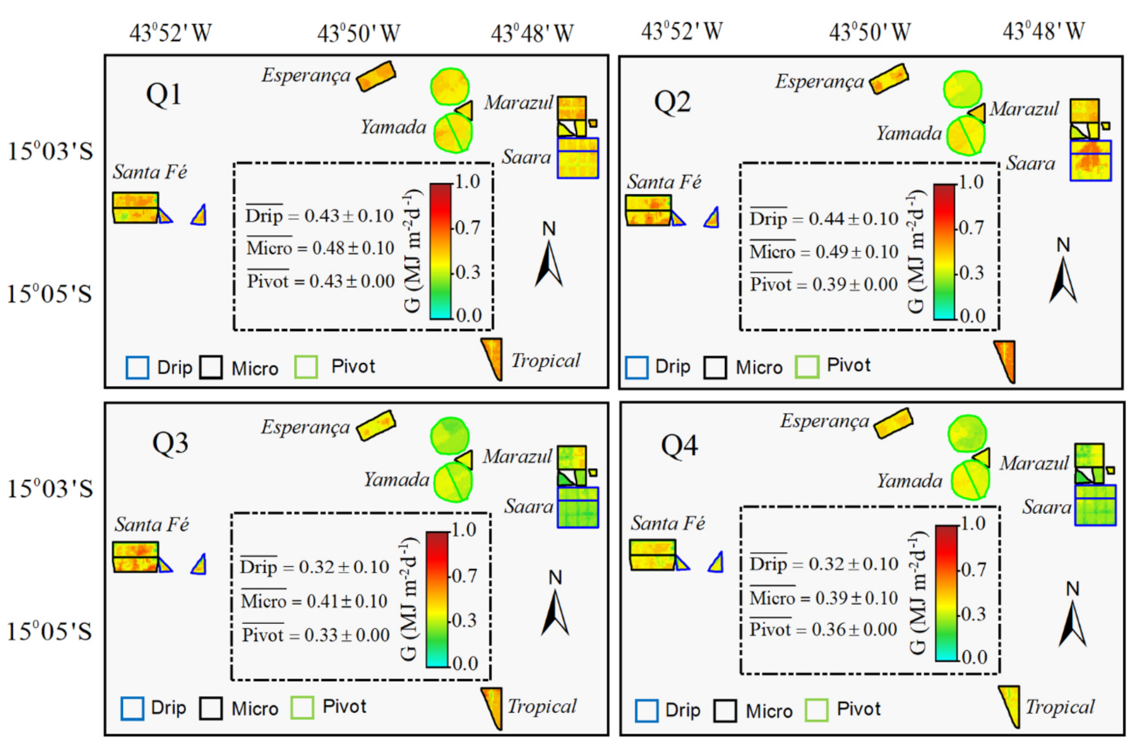

Fig. 7. Spatial distribution averages, and standard deviations (SD), for the soil heat flux (G) quarterly values. Blue, black, and green contour lines represent lemon orchards irrigated by drip, micro sprinklers, and pivot irrigation systems, respectively, inside the commercial farms from Table 2. Q1– First quarter (January to March); Q2 – Second quarter (April to June); Q3 – Third quarter (July to September); Q4 – Fourth quarter (October to December). (For interpretation of the references to colour in this figure legend, the reader is referred to the web version of this article.)

Table 10
Average quarterly values and standard deviations (SD) for soil heat flux (G), in drip, micro sprinkler, and pivot irrigated lemon orchards of each studied commercial farm, in the semi-arid region of São Francisco river basin, northern Minas Gerais state (MG), Southeast Brazil.

Farm/Irrigation system	Soil heat flux - G ($MJ\ m^{-2}\ d^{-1}$)				
[a]ES	[b]Q1	Q2	Q3	Q4	Year
Micro Sprinkler	0.51 ± 0.05a	0.47 ± 0.06a	0.41 ± 0.05a	0.44 ± 0.04b	0.46 ± 0.05
YA					
Micro Sprinkler	0.44 ± 0.04a	0.47 ± 0.03a	0.37 ± 0.03a	0.38 ± 0.03a	0.41 ± 0.03
Pivot	0.43 ± 0.04a	0.39 ± 0.04a	0.33 ± 0.04a	0.36 ± 0.04a	0.38 ± 0.03
SF					
Drip	0.42 ± 0.11a	0.41 ± 0.11a	0.35 ± 0.11a	0.34 ± 0.07a	0.38 ± 0.10
Micro Sprinkler	0.46 ± 0.09a	0.46 ± 0.10a	0.45 ± 0.13a	0.40 ± 0.09a	0.44 ± 0.09
SA					
Drip	0.43 ± 0.05a	0.46 ± 0.10a	0.28 ± 0.04a	0.30 ± 0.04a	0.37 ± 0.04
MA					
Micro Sprinkler	0.46 ± 0.07a	0.44 ± 0.06a	0.33 ± 0.08a	0.31 ± 0.06a	0.39 ± 0.06
TR					
Micro Sprinkler	0.55 ± 0.05b	0.59 ± 0.06b	0.51 ± 0.07b	0.42 ± 0.05b	0.52 ± 0.05

[a] ES – Esperança; YA – Yamada; SF – Santa Fé; SA – Saara; MA – Marazul; and TR – Tropical
[b] Q1– First quarter (January to March); Q2 – Second quarter (April to June); Q3 – Third quarter (July to September); Q4 – Fourth quarter (October to December). G rates with the same letter in each column indicate no significant differences from each other at 5% (pairwise comparisons using the Tuckey HSD post-hoc test performed for each quarter).

Table 11
Average quarterly values for the soil heat flux (G) to net radiation (R_n) ratios, in drip, micro sprinkler, and pivot irrigated lemon orchards, in the semi-arid region of the São Francisco river basin, northern Minas Gerais state (MG), Southeast Brazil.

Quarter/Irrigation System	Q1[a]	Q2	Q3	Q4	Year
Drip	0.04	0.05	0.04	0.03	0.04
Micro Sprinkler	0.04	0.06	0.05	0.04	0.05
Pivot	0.04	0.05	0.04	0.03	0.04

[a] Q1– First quarter (January-March); Q2 – Second quarter (April-June); Q3 – Third quarter (July-September); Q4 – Fourth quarter (October-December).

$$WD = ET_p - ET \quad (18)$$

$$WP_{ET} = \frac{Y_a}{ET} \quad (19)$$

where RET is the relative evapotranspiration, WD the water deficit (mm), WP_{ET} the water productivity based on ET ($kg\ m^{-3}$), and Y_a is the actual lemon yield (kg).

To retrieve ET_p in farms with both drip and micro sprinkler irrigation systems, weight averages for each farm according to the areas under these systems were performed:

$$ET_{p_{Farm}} = \frac{ET_{p_{Drip}} w_{Drip} + ET_{p_{Micro}} w_{Micro}}{w_{Drip} + w_{Micro}} \quad (20)$$

where $ET_{p_{Farm}}$, $ET_{p_{Drip}}$, and $ET_{p_{Micro}}$, are the potential evapotranspiration for a specific farm (subscript *Farm*), for drip irrigated areas (subscript *Drip*), and for micro sprinkler irrigated (subscript *Micro*) areas, respectively; while w_{Drip} and w_{Micro} are the percentages of areas for each irrigation system.

3. Results

3.1. Weather drivers

Fig. 3 shows the fortnightly values, during the year 2015, for totals of precipitation (P) and reference evapotranspiration (ET_0); and for the mean daily global solar radiation (R_G) and air temperature (T_a), in terms of Days of the Year (DOY).

The highest rainfall amounts occurred at the beginning of the year, when the fortnightly P totals were above 50 mm, during the second half of February (DOY 046–059). The driest periods, with some absence of rains, were from DOY 150–255 (end of May to the first half of September). Considering the annual timescale, P was 318 mm yr^{-1}, concentrated in the first and last three months. The highest ET_0 rates

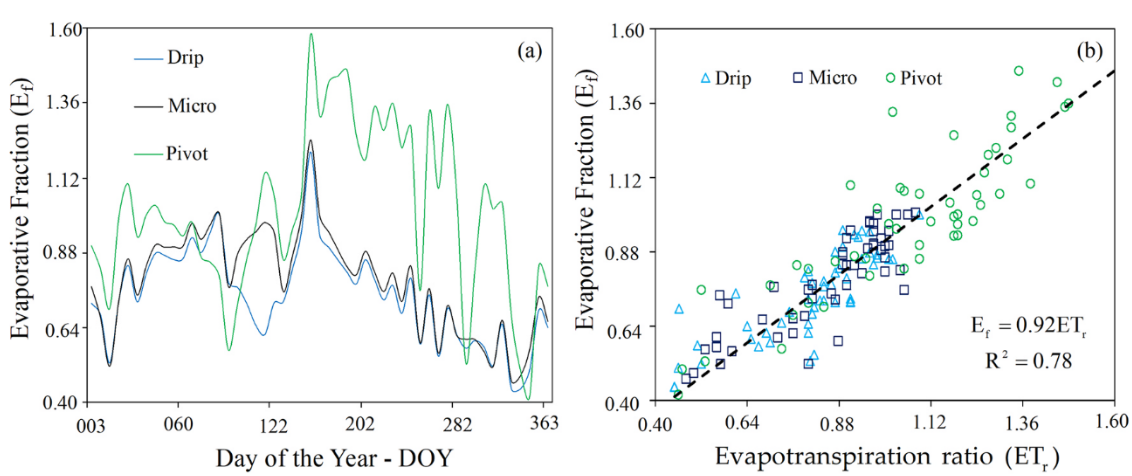

Fig. 8. Soil moisture indicators for lemon orchards under drip (*Drip*), micro sprinkler (*Micro*), and pivot (*Pivot*) irrigation systems in the semi-arid region of the São Francisco river basin, northern Minas Gerais state (MG), Southeast Brazil: (a) Fortnightly values of evaporative fraction (E_f); (b) Relationship between E_f and the evapotranspiration ratio (ET_r).

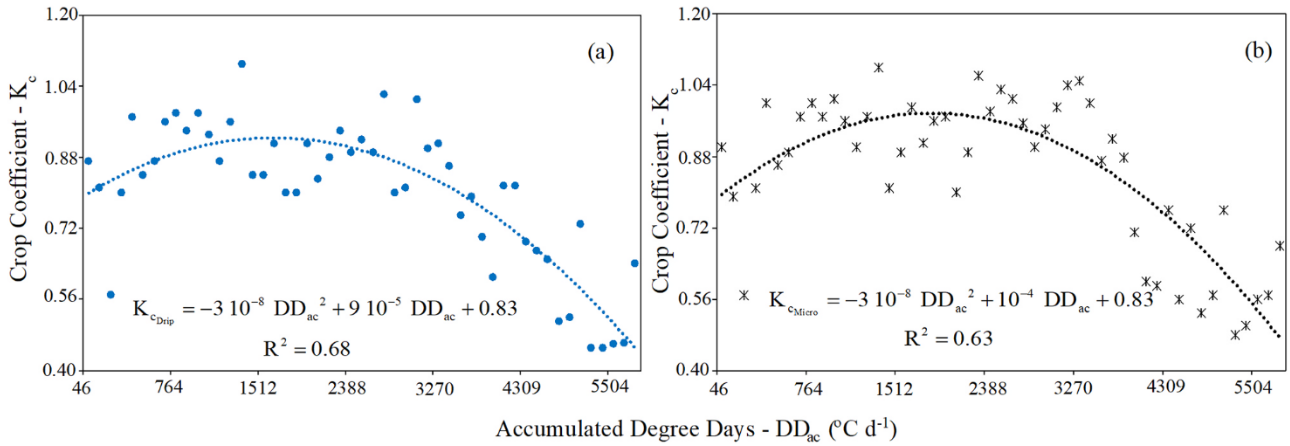

Fig. 9. Models for estimating single lemon crop coefficients (K_c) in the semi-arid region of the São Francisco river basin, northern Minas Gerais (MG) state, Southeast Brazil. (a) Drip irrigated orchards (*subscript Drip*); (b) Micro sprinkler irrigated orchards (*subscript Micro*).

occurred at the end of the year, with fortnightly totals higher than 80 mm, from October (DOY 274) to December (DOY 365), when there was a peak of 107 mm; while the lowest ones, below 60 mm, were from May to the first half of August (DOY 120–227). Regarding the annual timescale, ET_0 was 1670 mm yr^{-1}.

The highest R_G levels were from January to the first half of April (DOY 001–105), and between August and December (DOY 213–265), when the fortnightly values were higher than 22.5 MJ m^{-2} d^{-1}, dropping to around 18.5 MJ m^{-2} d^{-1} in the middle of the year, from DOY 121–196 (May-July). Considering the annual timescale, R_G averaged 20.2 MJ m^{-2} d^{-1}. The lowest T_a fortnightly values, below 24.0 °C, occurred in July (DOY 182–212), while the highest ones, above 29.0 °C, were from the second half of October (DOY 288) to the end of November (DOY 334). Regarding the annual timescale T_a averaged 26.0 °C.

3.2. Energy balance assessments

To follow the rainfall water availability and atmospheric demands along the year, the energy and water balance assessments were carried out in quarter periods, as in the Brazilian semi-arid region there are no well-defined four seasons, being restrict to dry and wet periods along the year.

Fig. 4 presents the spatial distribution, averages, and standard deviations (SD), of the R_n quarterly values (each three months), during the year 2015, for the lemon orchards irrigated by drip, micro sprinkler, and pivot systems, in the commercial farms from Table 2.

Table 4 shows the average quarterly values and SD for R_n in lemon orchards of each studied commercial farm, irrigated by drip, micro sprinkler, and pivot systems, together with the results of the pairwise comparison, using the Tuckey HSD post-hoc test performed at the 5% significance level for each quarter.

According to the Tuckey HSD test for each quarter, some differences on R_n values at the 5% significance level were found among irrigations systems, with higher values for micro sprinkler orchards in ES farm, in Q2 (April to June) and Q4 (October to December); SF farm, in Q3 (July to September) and Q4 (October to December); and TR farm, from Q1 (January to March) to Q4 (October to December).

The quarterly R_G average values from Fig. 3, resulted in 22.0, 19.5, 17.5, and 22.1 MJ m^{-2} d$-^{1}$, for Q1 (January-March), Q2 (April-June), Q3 (July–September), and Q4 (October–December), respectively. The corresponding R_n averages (Fig. 4) ranged from 7.90 MJ m^{-2} d^{-1} under drip irrigation system in Q3 (July–September) to 11.00 MJ m^{-2} d^{-1} for micro sprinkler irrigation system in Q1 (January to March).

These radiation values resulted in average R_n/R_G quarterly ratios for each irrigated system showed in Table 5.

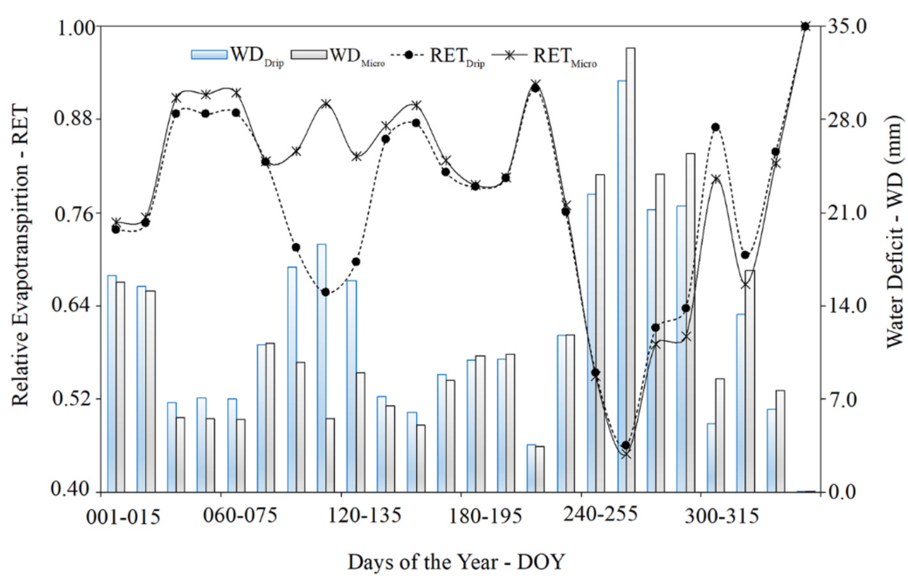

Fig. 10. Fortnightly values of irrigation performance indicators (IPI) for lemon orchards in terms of Days of the Year (DOY): water deficit (WD) and relative evapotranspiration (RET), for drip (*subscript Drip*) and micro sprinkler (*subscript Micro*) irrigation systems in the semi-arid region of the São Francisco river basin, northern Minas Gerais state (MG), Southeast Brazil.

Table 12
Irrigation performance indicators (IPI) for localized irrigated (drip and micro sprinkler systems) lemon orchards in the semi-arid region of the São Francisco river basin, northern Minas Gerais state (MG), Southeast Brazil. Actual (ET) and potential (ET_p) evapotranspiration; evapotranspiration ratio (ET_r); relative evapotranspiration (RET); water deficit (WD); actual yield (Y_a); and water productivity based on ET, on physical (WP_{ET}) and monetary ($WP_{ET\$}$) terms.

IPI[a]/Farms[b]	ET (m^3)	ET_p (m^3)	ET_r (-)	RET (-)	WD (m^3)	Y_a (ton)	WP_{ET} (kg m^{-3})	$WP_{ET\$}$ (US$ m^{-3})
ES	302,049	302,049	0.81	1.00	0	576	1.90	0.48
YA	129,848	150,063	0.73	0.87	20,215	333	2.60	0.65
SF	538,582	675,812	0.67	0.80	137,230	1554	2.90	0.73
SA	547,255	713,009	0.62	0.77	165,753	1948	3.60	0.90
MA	328,889	393,762	0.71	0.84	64,873	753	2.30	0.58
TR	242,403	245,072	0.83	0,99	2669	378	1.60	0.39

[a] IPI – Irrigation performance indicators
[b] Farms: ES – Esperança; YA – Yamada; SF – Santa Fé; SA – Saara; MA – Marazul; and TR – Tropical

The R_n/R_G ratios ranged from 43% in Q2 – April to June (Pivot systems) to 50% in Q1 – January to March (drip and pivot systems). However, at the annual scale all irrigation systems presented a fraction of 47% of R_G transformed into R_n.

From Fig. 4 and Tables 4 and 5, in general, there were no strong distinctions among the R_n pixel values, regarding the irrigation systems at the annual scale. Although the R_n spatial variations being small, with the SD values ranging from 1% (micro sprinkler and pivot) to 2% (drip) of the mean values (Table 4), drip systems promoted more irregular soil moisture, as wet bulbs are more concentrated to the root-zones under this irrigation method.

The spatial and temporal pixel differences among the irrigation systems under the distinct root-zone moisture conditions along the year, should be more perceived when considering the R_n partitions into λE, H, and G. According to Consoli and Vanella (2014), accurate knowledge of the R_n partitioning is needed to develop reliable tools for studying short-term or long-term processes within agricultural crop ecosystems, which are particularly fragile under water scarcity conditions.

Fig. 5 shows the spatial distribution, averages, and standard deviations (SD), of the λE quarterly values, during the year 2015, for the lemon orchards irrigated by drip, micro sprinkler, and pivot systems, on the commercial farms from Table 2.

Table 6 shows the averages quarterly values and SD for λE in lemon orchards of each studied commercial farm, irrigated by drip, micro sprinkler, and pivot systems, together with the results of the pairwise comparison, using the Tuckey HSD post-hoc test performed at the 5% significance level for each quarter.

According to the Tuckey HSD test for each quarter, significant differences on λE values were found among irrigations systems, with higher values in the ES farm, under micro sprinkler irrigations, in all quarters; in YA farm, under Pivot irrigation, in all quarters; and in TR farm, in Q1 (January to March), Q2 (April to June), and Q4 (October to December), under micro sprinkler irrigation.

Considering all analyzed irrigation systems, the highest λE rates occurred in Q1(January to March) and Q2 (April to June), above 9.00 MJ m^{-2} d^{-1} for micro sprinkler and pivot irrigation systems. The average λE quarterly values ranged from 4.85 to 9.45 MJ m^{-2} d^{-1}, for drip (Q3 – April to June) and pivot (Q1 – January March) irrigation systems, respectively. At the annual scale, λE averaged 6.26 MJ m^{-2} d^{-1}, 7.63 MJ m^{-2} d^{-1}, and 9.02 MJ m^{-2} d^{-1}, under drip, micro sprinkler, and pivot irrigation systems, respectively.

Table 7 shows the average quarterly values for the λE to R_n ratios in lemon orchards irrigated by drip, micro sprinkler, and pivot systems.

The λE/R_n values were above 100% during Q2 (April to June) and Q3 (July to September), in lemon orchards irrigated by pivot systems. The lowest ones, with quarterly average below 0.55, occurred in Q4 (October to December) for drip irrigation systems, at the end of the climatically driest period and increasing atmospheric demand in the study region (see also P and ET_0 values from Fig. 3).

Fig. 6 presents the spatial distribution, averages, and standard deviations (SD), of the H quarterly values, during the year 2015, for the lemon orchards irrigated by drip, micro sprinkler, and pivot systems, in the commercial farms from Table 2.

Table 8 shows the average quarterly values and SD for H in lemon orchards of each studied commercial farm, irrigated by drip, micro sprinkler, and pivot systems, together with the results of the pairwise comparison, using the Tuckey HSD post-hoc test performed at the 5% significance level for each quarter.

According to the Tuckey HSD test for each quarter of the year, significant differences on H values were also found among irrigations systems, with higher values for drip systems in SF farm for all quarters, in micro sprinkler systems of YA (Q1 – January to March, and Q4 – October to December) and MA (Q4 – October to December) farms; and also for the pivot systems of YA farm during Q2 (April–June). In this last case, negative values indicated heat horizontal advection from the drier vicinity areas to irrigated orchards.

The highest H rates occurred in Q4 (October to December), above 4.50 MJ m^{-2} d^{-1}, for localized irrigation systems (drip and micro sprinkler irrigated orchards). The quarterly averages ranged from −1.69 MJ m^{-2} d^{-1} (Pivot) in Q3 (April–June) to 4.79 MJ m^{-2} d^{-1} (drip) in Q4 (October to December). The largest positive H for the drip irrigated lemon orchards happened at the end of the climatically driest period under the highest atmospheric demand conditions (see also Fig. 3). At the annual scale, H averaged 2.82 MJ m^{-2} d^{-1}, 1.53 MJ m^{-2} d^{-1}, and 0.10 MJ m^{-2} d^{-1}, for drip, micro sprinkler, and pivot irrigation systems, respectively.

Table 9 shows the average quarterly values for the H to R_n ratios in lemon orchards irrigated by drip, micro sprinkler, and pivot systems.

Energy partition into H (H/R_n) was above 43% during Q4 (October to December), for drip irrigated lemon orchards. The negative average H/R_n values occurred under pivot irrigation areas from Q2 (April to June) to Q3 (July to September), but also under micro sprinkler irrigation systems in Q2 (April to June). The most negative H/R_n ones in pivot irrigated areas, during Q3 (July to September), evidenced a high contribution of an extra horizontal energy transfer from the drier and hotter *Caatinga* species to the moistier and colder irrigated lemon orchards in YA farm, during this time of the year.

Fig. 7 shows the spatial distribution averages, and standard deviations (SD), of the G quarterly values, during the year 2015, for the lemon orchards irrigated by drip, micro sprinkler, and pivot systems, on the commercial farms from Table 2.

Table 10 shows the average quarterly values and SD for G in lemon orchards of each studied commercial farm, irrigated by drip, micro sprinkler, and pivot systems, together with the results of the pairwise comparison, using the Tuckey HSD post-hoc test performed at the 5% significance level for each quarter.

According to the Tuckey HSD test for each quarter, some differences on G values were found among irrigations systems with higher values in ES farm only in Q4 (October to December), but in all quarters in TR farm for micro sprinkler irrigation systems.

The highest G average quarterly value, above 0.55 MJ m^{-2} d^{-1}, occurred in Q2 (April to June) for micro sprinkler irrigated lemon orchards in TR farm, while the lowest one, bellow 0.30 MJ m^{-2} d^{-1} occurred in Q3 (July to September), in SA farm under drip irrigated orchards.

Table 11 shows the average quarterly values of the G to R_n ratios for lemon orchards irrigated by drip, micro sprinkler, and pivot systems.

The largest G/R_n values were in Q2 (April to June), around 6%, for micro sprinkler irrigation systems and 5% for both drip and pivot irrigated areas, while the lowest ones happened in Q4 (October to December) corresponding to average G/R_n ratios of 4% (micro sprinkler systems) and 3% (drip and pivot systems). However, at the annual scale, G/R_n averaged only 5% (micro sprinkler system) and 4% (drip and pivot systems).

3.3. Irrigation performance assessments

Considering the λE rates from Fig. 5 in terms of ET, at the annual scale, pixel values averaged 2.6 mm d^{-1}, 3.1 mm d^{-1}, and 3.7 mm d^{-1}, respectively for drip, micro sprinkler, and pivot irrigated lemon orchards. Thus, among the irrigation systems, pivot was the one with the highest ET rates. To analyze the root-zone moisture levels, the remote sensing indicators firstly considered were the evapotranspiration ratio (ET_r) and the evaporative fraction (E_f), resulting from applications of the Eqs. (10) and (13), respectively.

Fig. 8 presents the E_f fortnightly values (Fig. 8a), in terms of Days of the Year (DOY), and its relationship with ET_r (Fig. 8b), for lemon orchards irrigated by drip, micro sprinkler, and pivot systems, along the year 2015.

The average E_f ranged from 0.44 to 1.20, 0.47–1.24, and 0.42–1.58, for the drip, micro sprinkler, and pivot irrigation systems, respectively (Fig. 8a). The highest E_f values occurred between DOY 154 and 163 (first half of June), from the FG to HP phenological stages (see also Table 1), with few occasions with low E_f, when it values dropped below 0.60 for drip and micro sprinkler irrigation systems after DOY 282. On the other hand, the pivot E_f values often above 1.00 indicated the highest water consumption among systems, strongly evidenced by its curve on Fig. 8a, after the first half of May (DOY 131). Fig. 8b shows that, for irrigated lemon orchards, E_f values were around 92% of those for ET_r, corresponding to an ET_r range from 0.30 to 0.90, under localized irrigation (drip and micro sprinkler systems), and between 0.30 and 1.30 for the pivot irrigated orchards.

Because lemon orchards under pivot irrigation systems use too much water, according to their E_f and ET_r values, these systems are not recommended under the water scarcity scenarios of the Brazilian semi-arid region. Fig. 9 shows the models to estimate K_c as a function of DD_{ac}, for the recommended drip (Fig. 9a) and micro sprinkler (Fig. 9b) irrigation systems under these conditions (Teixeira et al., 2014a). Similarly, Rallo et al. (2017), to infer the phenological stages of drip irrigated orange orchards, used site-specific polynomial equation to determine K_c as a function of the measured canopy fractional cover to determine water requirements under the semi-arid conditions of Spain..

Points above the curves from Fig. 9 indicate high contributions of soil evaporation while the ones bellow represent conditions of ET lower than ET_p. Then, both conditions are eliminated when estimating the crop water requirements by applying the polynomial equations. For drip irrigation systems, the modelled K_c values ranged from 0.37 to 0.90, averaging 0.78, while the corresponding ranges and average for the micro sprinkler irrigation systems were respectively 0.43–0.92, and 0.81. By crossing Table 1 and Fig. 9, the maximum K_c values occurred during the transition from F to FG phenological stages, between March and April, and from September to October; while the minimum ones were from November to December, during the HP phenological stage.

Fig. 10 shows the fortnightly values for the irrigation performance indicators (IPI); the water deficit (WD) and the relative evapotranspiration (RET), for drip (*subscript Drip*) and micro sprinkler (*subscript Micro*) irrigated lemon orchards, in terms of DOY.

From Fig. 10, in general, RET values were higher than 0.60, except from the start of September (DOY 240) to the end of October (DOY 300), when it dropped below 0.50 and the fortnightly WD values increased above 20.0 mm, from F to FG phenological stages (see also Table 1). The annual RET and WD values for drip and micro sprinkler irrigation systems were 0.77 and 293 mm yr^{-1}, and 0.79 and 278 mm yr^{-1}, respectively.

On the annual scale, the IPI values are summarized in Table 12, for each studied lemon producer farms, by weighting drip and micro sprinkler irrigated areas for each one according to Eq. (20).

According to the previous Table 2, among the producer farms, the largest lemon cropped area is for micro sprinkler irrigation, with a total of 122.01 ha. The orchards are drip irrigated only in SA and SF farms, with 53.93 ha and 6.93 ha, respectively. For total ET, data on cropped area for each farm allowed transforming mm into m^3 of water, to illustrate the magnitude of water withdrawals from the São Francisco River, resulting in maximum and minimum rates for SA and YA farms, respectively. As for ET, the highest and lowest ET_p values were also for SA and YA farms, respectively. Regarding the root-zone moisture levels, the best conditions were for TR and ES farms, with ET_r above 0.80, not coinciding with the largest evapotranspiration rates.

Data on Prod together with the monetary returns, allowed water productivity assessments on both physical (WP_{ET}) and economical ($WP_{ET\$}$) terms, for each studied lemon producer farm. The WP_{ET} ranged from 1.60 to 3.60 kg m^{-3}, yielding monetary values ($WP_{ET\$}$), between 0.39 and 0.90 US\$ m^{-3}. The highest values were for SA farm, with 100% of its lemon cropped area being drip irrigated, while the lowest ones were for TR farm, under only micro sprinkler irrigation system.

4. Discussion

Considering the climatic water balance (Fig. 3), P was more variable than ET_0, with absence of rain in the middle of the year, agreeing with the long-term tendencies, of the study region (Lumbreras et al., 2014). However, scarce rainfall was registered, even during the rainy season, from DOY 060–120 (March to April), with fortnightly P values dropping below 4% of ET_0. At the annual scale P was 37% of the climatological value (560 mm yr^{-1}) and only 19% of ET_0 in 2015, indicating a strong dry year regarding the long-term conditions of the region. The highest R_G and T_a values were at the end of the year, at the sun's zenith position and under low cloud cover, while the lowest ones were in the middle of the year, winter solstice in the southern hemisphere. Thus, the highest lemon water consumptions and photosynthesis activities occurred in the first (Q1, January-March) and fourth (Q4, October-December) quarters of the year.

Regarding the energy balance, R_n was strongly influenced by the R_G levels, with the lowest values in the middle of the year, all quarters having low SD, representing only 1–3% of the average values (Fig. 4 and Table 4). An average R_n/R_G fraction of 47% (see Table 5) agrees with other remote sensing measurements in different agroecosystems of the Southeast (Teixeira et al., 2017a; Silva et al., 2018), and Northeast (Teixeira et al., 2017b) Brazil, as well as with field measurements in an olive orchard under the Mediterranean semi-arid climate conditions (Ramírez-Cuesta et al., 2019b). However, the annual R_n value of 9.45 MJ m^{-2} d^{-1} in the current study was much lower than that of 15.00 MJ m^{-2} d^{-1} reported by Villalobos et al. (2009) for drip-irrigated oranges growing in the semi-arid conditions of Spain.

The highest λE rates in Q1 – January to March (Fig. 5 and Table 6) were due to the coupled effects of rains and irrigation water applied, which increased the root-zone moisture, under high atmospheric demands (see also Fig. 3). The λE range, between 4.98 MJ m^{-2} d^{-1} (Drip irrigation in Q3 – April to June) and 9.45 MJ m^{-2} d^{-1} (Pivot irrigation in Q1 – January to March), encompassed the values from 4.90 to 9.40 MJ m^{-2} d^{-1}, reported for olive orchards (Ramírez-Cuesta et al., 2019b), and drip irrigated orange (1.80–9.50 MJ m^{-2} d^{-1}) (Consoli and Papa, 2013), both studies under the Mediterranean semi-arid conditions. Differently from R_n, the λE spatial variations are clear, with higher SD values. From Q2 (April to June) to Q3 (July to September), some λE pixel values were higher than R_n in the well-irrigated lemon parcels meaning horizontal heat advection, mainly under pivot irrigation systems, promoting an average $λE/R_n$ higher than 1.00 (Table 9). This additional horizontal energy was also verified in drip irrigated orange orchards, under the Mediterranean semi-arid conditions of Sicily, Italy (Consoli and Papa, 2013). The λE rates were most affected by variations on root-zone moisture levels, which in turn depended on the weather conditions, but also the type of irrigation system which affects ET partitions into transpiration and soil evaporation (Fandiño et al., 2012; Consoli and Vanella, 2014; Rosa et al., 2016; Longo-Minnolo et al., 2020). Our average R_n partition into λE of 66% for drip-irrigated lemon orchards (Table 7) was higher than that of 38% reported by Villalobos et al. (2009) for drip-irrigated orange orchards in the semi-arid region of Spain, which differences may be related to distinct species and environmental conditions but also to irrigation management.

From the H spatial variations (Fig. 6 and Table 8), there were some negative pixel values, promoting an average H/R_n ratio lower than 0,00 in Q2 (April to June) and Q3 (July to September), mainly in lemon orchards under the pivot irrigation systems (Table 9). The magnitudes of the negative H values indicate the degree of horizontal heat advection, what was more noticed in Q3 (July to September), highlighting the stronger cooling effects of the pivot irrigation systems, while higher positive H rates under drip irrigation lemon orchards in Q4 (October to December) indicated strong warming effects. The absence of negative H values in Q1 and Q4 is that rainfalls promoted more uniform root zone moisture to the irrigated orchards and natural vegetation. Negative H values from remote sensing measurements, up to −4.00 MJ m^{-2} d^{-1} were also reported in mixed agroecosystems in Southeast Brazil (Teixeira et al., 2017a). From a field energy balance study, Consoli and Papa (2013) reported negative H/R_n values, but with quarterly values, representing up to 47% of R_n in a drip-irrigated orange orchard, growing in the Mediterranean semi-arid region, similar to our H/R_n ratio of 43% in Q4 (October to December) for drip-irrigated lemon orchards (Table 9). From water balance measurements under the semi-arid conditions of southern Iran, Jamshidi et al (2020), also found high horizontal heat advection in a drip-irrigated orange orchard. H values for drip-irrigated lemon orchards in our study region were 45% of those for λE much lower than those reported by Villalobos et al. (2009), who found H being 155% of λE from field energy balance measurements in drip-irrigated orange orchards under the semi-arid conditions of Spain. Average K_s of 0.16 indicated some of water stress in this last study, what reinforce that one of the reasons for differences in energy partition should be related to irrigation management.

Small spatial and temporal variations on G happened along the year, and among irrigated lemon orchards (Fig. 7 and Table 10). The partition of R_n on G was of the lowest magnitude, when comparing with the other energy balance terms (Table 11). According to the SD values, G spatial variation was small and independent of the irrigation system, ranging from 0.0 to 0.1 MJ m^{-2} d^{-1}. Both, G magnitude and SD small values testified that this energy balance component can be neglected at daily timescale in semiarid regions (Consoli and Papa, 2013; Teixeira et al. 2017b). Vilallobos et al. (2009), measuring G with soil heat flux plates during two years in an irrigated orange orchard, under the semi-arid conditions in Spain, registered average G values being 3% of R_n, a little lower than ours from Table 11. Teixeira et al. (2008b), throughout field measurements in drip and micro sprinkler irrigated vineyards and micro sprinkler irrigated mango orchards also found near zero G daily values in the Brazilian semi-arid region.

At the annual timescale, the $λE/R_n$ and H/R_n ratios for drip, micro sprinkler, and pivot irrigated lemon orchards, were respectively 0.66 and 0.30; 0.79 and 0.16; and 0.95 and 0.01, evidencing the largest available energy being used for ET in all analyzed irrigation systems. These distinct energy partitions are related to the different water use for transpiration and evaporation (Fandiño et al., 2012; Consoli and Vanella, 2014; Rosa et al., 2016; Longo-Minnolo et al., 2020). For example, for pivot system, there is much more evaporation from both near-surface air and soil, what can explain the highest $λE/R_n$ ratios (and therefore the lowest H/R_n) when compared with the localized irrigation systems (drip and micro sprinkler systems).

Although knowledge about the available energy partition in irrigated crops being strongly relevant for agriculture, it is restricted to academic readers, being of difficult understanding by water managers as the end users. For operational interpretations, simple irrigation performance indicators (IPI) are used in the current paper, resulted from the energy and water balance computations. The IPI ranges would facilitate water management by irrigation advisors and technicians, while promoting a more efficient use of water resources (Cancela et al., 2019).

After transforming the λE pixel values (Fig. 5) into ET, we assessed the performance of the drip, micro sprinkler, and pivot irrigation systems inside the farms described in Table 2 throughout IPI values. One of the reasons of varying ET rates might be caused by different areas of soil covered by each of these systems (Villalobos et al., 2009). Pivots wet more surface than drips and micro sprinklers. For instance, considering a difference of 1.0 mm d^{-1} between the pivot and drip irrigation systems, and the pivot total area of 46.28 ha in Yamada (YA) farm (see Table 2), this means an annual ET difference of 168,922 m^3 yr^{-1}.

Consoli and Papa (2013), through field energy balance measurements in a drip irrigated orange orchard, found an average ET rate of 2.4 mm d^{-1}, under the Mediterranean semi-arid conditions. Yang et al. (2003) reported similar rates from lysimeter measurements, also in drip irrigated oranges but growing in Japan. Lysimeter measurements in lemon orchard in Southeast Brazil, retrieved an average ET value of 2.9 mm d^{-1} (Junior et al., 2008). The average values from these previous studies are inside of the range for the localized irrigated lemon orchards in the current study (daily averages of 2.0 mm d^{-1} and 3.4 mm d^{-1}, respectively for drip systems in Q3 – July to September, and micro sprinkler systems in Q1 – January to March). However, in southern Italy, Consoli and Vanella (2014), using different remote sensing methods, found higher average daily ET, ranging from 3.1 to 4.1 mm d^{-1} in drip irrigated oranges. In the same region, crop, and irrigation system, Longo-Minnolo et al. (2020), also reported a higher average ET value of 3.8 mm d^{-1}, coupling remote sensing and weather data. On the other hand, in central India, Panigrahi and Srivastava (2016) found a lower average ET value of 1.8 mm d^{-1}, from water balance measurements. These distinct ET values in Italy and India regarding the current study, may be attributed to differences in atmospheric demands and irrigation managements, when compared to those for the Brazilian semi-arid conditions.

In general, lemon orchards in the Brazilian semi-arid region were at good root-zone moisture but the highest E_f and ET_r values (Fig. 8) were for the pivot systems, while the lowest ones happened in drip irrigated areas. The reason is that besides pivot system spread water over a large portion of soil and the air close to the orchards, favoring evaporation, this irrigation system also modifies the microclimate, while drip systems restrain the wet bulb close to the root zones, reducing the partition of ET into evaporation and increasing the partition of R_n into H. According to Zhou and Zhou (2009), air humidity and the available energy, were the most important variables for the root-zone moisture variations in a reed marsh in Northeast China. However, E_f and ET_r values in plants under non-optimum root--zone moisture conditions, are also influenced by the stomatal regulation (Mata-González et al., 2005; Mateos et al., 2013).

The maximum single K_c values represented by the peak of the polynomial curves in Fig. 9 (0.90 and 0.92, for drip and irrigation systems, respectively) were higher than the single K_c ones tabulated for citrus by Allen et al. (1998). One of the reasons of the lower values for drip irrigation systems in comparison with the micro sprinkler ones, should be its higher partition into transpiration, lowering the evaporation coefficient (K_e). Longo-Minnolo et al. (2020), analyzing irrigation strategies in citrus orchards from remote sensing and agro-meteorological data in Southern Italy, reported K_c values ranging from 0.56 to 0.67 for drip-irrigated oranges, varying according to treatments as indicators of transpiration activities, also bellow the FAO tabled values (Allen et al., 1998). Differences on K_c values from the recommended FAO tabulated values were also found by Consoli and Papa (2013) from field measurements in an irrigated orange orchard under the Mediterranean semi-arid conditions, resulting in a K_c range from 0.20 to 1.10, averaging 0.68. Also, for irrigated orange orchard, K_c

values averaging 0.91 and 0.75 were reported, during respectively summer and winter seasons in Japan, respectively (Yang et al., 2003). On the other hand, in Southeast Brazil, Junior et al. (2008) found K_c values from 0.82 to 1.18 from lysimeter measurements in an irrigated lemon orchard, like the range of our K_c values.

From soil water balance measurements under the semi-arid conditions of southern Iran, Jamshidi et al. (2020) reported K_c range from 0.67 to 0.96 in a drip-irrigated orchard under different deficit irrigation strategies, higher than our results for drip-irrigated lemon orchards. According to these authors, discrepancies in the reported K_c values are due to climatic differences (Yang et al., 2003; Niziński et al., 2017), irrigation management (Zitouna-Chebbi et al., 2015), plant physical and biological features (Consoli et al., 2006; García-Tejero et al., 2011; Consoli and Papa, 2013), and soil evaporation rates (Maestre-Valero et al., 2017), highlighting the need for local calibrations (Rana et al., 2005; Villalobos et al., 2009, 2013). As, one of the reasons for K_c differences may be attributed to climate and phenological stages, the models relating K_c and DD_{ac} depicted in Fig. 9 can be used to calibrate the effect of the thermal effects, when aiming irrigation performance assessments and water management (Teixeira et al., 2014a). However, if some water stress is desired during specific phenological stages, to improve water productivity (Panigrahi and Srivastava, 2016; Garcia--Tejero et al., 2010, 2019), a reduction coefficient (K_s) can be included in water management (Mateos et al., 2013; Rallo et al., 2017; Longo-Minnolo et al., 2020; Jamshidi et al., 2020).

Increasing on WD and decreasing on RET from DOY 240 (end of August) to 315 (first half of November), during the F to FG phenological stages in the current study (Fig. 10), may had affected the lemon yield, according to Panigrahi et al. (2016) and Garcia Tejero et al. (2010, 2019). These authors recommended reduction of irrigation water to a certain level, during the initial growth period and final fruit stages of citrus, to improve WP_{ET}. On the other hand, according to Jamshidi et al. (2020), some care should be taken with this reduction as water stress conditions could occur due to environmental or physiological stresses. The WD and RET differences between the drip and micro sprinkler irrigation systems, in mid-May (DOY 105–150), could be also attributed to gaps for recovering the soil moisture after rains in drip irrigated lemon orchards, compared with the micro sprinkler irrigated ones, which promote a high partition of ET into soil evaporation (Mateos et al., 2013, Longo-Minnolo et al., 2020).

From Table 12, it seems that a better water use is done in the SA farm, which could be taken as a reference farm in terms of irrigation performance in the study region. Thus, the best yield levels were achieved under drip irrigation, where some gaps happened between crop water consumption and crop water requirements. These findings agree with other authors (Garcia Tejero et al., 2010, 2019; Pedroso et al., 2014; Ballester et al., 2014; Chai et al., 2016; Robles et al., 2017; Jamshidi et al., 2020; Longo-Minnolo et al., 2020), who reported that some deficit irrigation in specific phenological stages of citrus orchards will favor yield and quality, while maximizing water savings in arid and semi-arid regions.

Rallo et al. (2017) emphasized that water-saving management strategies, such as regulated deficit irrigation (RDI) and partial root-zone drying (PRD), can contribute to increase citrus WP_{ET}. Under RDI, water is generally supplied at levels below full crop transpiration during specific periods of the growing season. PRD method involves the exposure of half of the roots system in a drying state, while the remaining roots are wetted (Hutton and Loveys, 2011; Romero-Conde et al., 2014). Previous studies proved that in citrus orchards, fruit drop is not very sensitive to soil water deficit applied during some periods of fruit growth and, if returning to the full water dosage for a sufficiently long period before harvesting (González-Altozano and Castel, 1999). More recent studies have proved that these strategies are promising techniques to increase citrus yield with water savings (Melgar et al., 2010; Hutton and Loveys, 2011; Ballester et al., 2013, 2014).

In central India, drip irrigation in orange orchards saved 30% irrigation water while enhancing yield by 50%, compared with basin irrigation (Panigrahi et al., 2012). In the same region and crop, Panigrahi and Srivastava (2016) demonstrated that reducing 20% and 40% of irrigation requirements, during the fruit growth periods, increased 18% on fruit yield with better quality, and 30% on WP_{ET} levels. Analyzing two years of water balance and yield of an orange orchard under different irrigation deficit strategies in the Iranian semi-arid, Jamshidi et al (2020), found significant differences among drip irrigation treatments (water applied at 45–100% of ET_0), with increases on yield as water applied increased, but till a certain degree, when yield and fruit size differences were not statistically significant. Consoli et al. (2017) studying the effects of the PRD technique on yield and fruit quality of young orange trees Eastern Sicily (Southern Italy), concluded that with trees irrigated at 50% of crop water requirements, fruit yield increased by 10–20%, without fruit quality reductions, improving WP_{ET} three times when compared with the full irrigation treatment.

Considering all assessed farms in the current study, ET was equivalent to more than 75% of ET_p, indicating, in general, enough irrigation water supplies, however, the large WP_{ET} range (Table 12), highlighted rooms for irrigation water management improvements. Panigrahi and Srivastava (2016), reported a WP_{ET} increase in a drip irrigated orange orchard in central India from 2.3 to 2.9 kg m^{-3} proportionally to water stress level. Improvements on WP_{ET} with deficit irrigation were also reported in a semi-arid region of Spain (Garcia Tejero et al., 2010, 2019). Considering the irrigation water applied ranging from 45% to 100% of ET_0 in the semi-arid of Iran, Jamshidi et al. (2020) reported WP_{ET} values for drip irrigated oranges from 2.0 to 3.0 kg m^{-3}. The authors recommended the treatment of irrigation water applied at 60 or 70% of ET_0 as the best option for minimizing the amount of water use while still maintaining the benefit of a good yield.

Although lemon $WP_{ET\$}$ values for the studied lemon orchards from 0.39 to 0.90 US\$ m^{-3}, being higher than those for corn in Southeast Brazil (0.34–0.68 US\$ m^{-3}) (Teixeira et al., 2014a), and other arable crops around the world (0.10–0.20 US\$ m^{-3}) (Sakthivadivel et al., 1999), they are much lower than those for table grapes (2.2 and 8.1 US\$ m^{-3}, respectively) and mangos (1.3 and 1.8 US\$ m^{-3}) in Northeast Brazil (Teixeira et al., 2009b). However, besides irrigation management and schedule, other issues are important to consider in $WP_{ET\$}$ assessments, as for example, the overall production costs, the rootstock/cultivar combinations, plant ages, spacings, and environmental differences (Germaná and Sardo, 2004; Panigrahi et al., 2012; Pedroso et al., 2014; Ballester et al., 2014; Panigrahi and Srivastava, 2016; Chai et al., 2016; Robles et al., 2017; Garcia Tejero et al., 2019; Teixeira et al., 2009b).

According to the current irrigation performance assessments, techniques about the use of regulated deficit irrigation strategies, in some phenological stages of lemon orchards are encouraged in the study region, aiming to maintain or improve lemon yield, while promoting water savings. Applications of the SAFER algorithm without the satellite thermal band improving spatial resolutions can contribute to these studies, being of great value for both researchers and advisors (Cancela et al., 2019). In addition, the algorithm implementation can also contribute to minimize conflicts among farmers and other water users, under the water scarcity conditions in semi-arid environments.

Although SAFER had been elaborated and validated with Landsat images in the Brazilian semi-arid regions, to replicate the method in other regions should require calibrations of the regression coefficients, mainly for Eq. (10), what can be done by remote sensing estimations of α_0, NDVI and T_0 together with field measurements of ET and ET_0. For ET one can apply energy or water balance methods, while for ET_0, weather data close to the experimental areas can be used (Venancio et al., 2021). The algorithm allows to overcome the limitations of energy balance models related to the lack of thermal data at high spatial/temporal resolution. In addition, the temporal upscaling process of ET values is avoided as daily ET values can be used directly (Consoli and Vanella, 2014).

The main limitations of remote sensing algorithms for water advisors are the availability of cloud-free satellite images, reliable agro-meteorological data, and the need of some radiation physic knowledges. However, the development of simple regressions as showed in Fig. 9 allow the water management based only on weather data. Having data on T_a and ET_0 it is possible to estimate lemon water requirements in any time of the year based on DD_{ac}, allowing applications of regulated deficit irrigation strategies incorporating the K_s coefficient in specific crop stages.

5. Conclusions

The joint use of Landsat 8 (L8) images and agrometeorological data made it possible to estimate the energy balance components for irrigation performance assessments in lemon orchards, under different irrigation systems, in the semi-arid region of the São Francisco river basin, northern Minas Gerais state, Southeast Brazil. The magnitude of the energy balance components varied spatially and temporally along the year, with the evaporative fraction above 1.00 and 1.30 for localized (micro sprinkler and drip systems) and pivot irrigation systems, respectively, from fruit growth to harvest peaks phenological stages.

Applications of the SAFER algorithm to L8 images identified different water fluxes from irrigated areas in lemon producer farms under distinct irrigations system. Due to high water use by pivot irrigation systems under the circumstances of water scarcity of the Brazilian semi-arid region, only localized irrigation systems were recommended, through the modeling of crop coefficient and estimations of crop water requirements.

Lower water consumptions were detected in lemon drip irrigated orchards with some degree of water deficit because the evapotranspiration (ET) process occurs on a limited extension close to the root zones wetted by the drippers, increasing the ET partition into transpiration. The use of drip irrigation systems with regulated deficit irrigation strategies are then encouraged when aiming at good lemon yield, while promoting water savings.

Besides the results of the current study being important for improving irrigation performance assessments and irrigation water management of lemon orchards in the study region, the success of these specific applications may allow the replication of the methods in citrus around the world, with probably the need of simple adjustments in the regression coefficients of the modelling equations.

CRediT authorship contribution statement

Antônio H. de C. Teixeira: was responsible for running the models, Conceptualizations, Energy balance and irrigation assessments, Writing the manuscript, Designing of figures, Result analyses, Software resources, Supervision, Project administration, Funding acquisition. **Janice F. Leivas:** Oversaw running of scripts, Download of Landsat 8 images, Formatting of the weather data, Methodology, Data curation, Editing of the manuscript. **Tiago B. Struiving:** Helped in geo referencing the lemon cropped areas, Crop yield information, Weather data processing, Result analyses. **João B. R. S. Reis:** Acted on review, Validation, Editing the manuscript, Weather data processing, Result analyses. **Fúlvio R. Simões:** Acted on review, Validation, Editing the manuscript, Weather data processing, Result analyses.

Funding

This research was funded by National Council for Scientific and Technological Development (in Portuguese: *Conselho Nacional de Desenvolvimento Científico e Tecnológico* - CNPq), grant numbers 404229/2013-1 and 446136/2015-8.

Acknowledgments

To CNPq, for the financial support to our projects on energy and water balances.

Conflicts of Interest

The authors declare no conflict of interest.

References

Allen, R.G., Pereira, L.S., Raes, D., Smith, M., 1998. Crop Evapotranspiration: Guidelines for Computing Crop Water Requirements. Food and Agriculture Organization of the United Nations, Rome, Italy.

Allen, R.G., Tasumi, M., Morse, A., Trezza, R., Wright, J.L., Bastiaanssen, W.G.M., Kramber, W., Lorite, I., Robison, C.W., 2007. Satellite-based energy balance for mapping evapotranspiration with internalized calibration (METRIC) - applications. J. Irrig. Drain. Eng. 133, 395–406.

Araujo, L.M., Teixeira, A.H. de C., Bassoi, L.H., 2019. Evapotranspiration and biomass modelling in the Pontal Sul irrigation scheme. Int. J. Remote Sens. 1, 1–13.

Ballester, C., Castel, J., Abd El-Mageed, T.A., Castel, J.R., Intrigliolo, D.S., 2014. Long-term response of 'Clementina de Nules' citrus trees to summer regulated deficit irrigation. Agric. Water Manag. 138, 78–84.

Ballester, C., Castel, J., Intrigliolo, D.S., Castel, J.R., 2013. Response of Navel Lane Late citrus trees to regulated deficit irrigation: yield components and fruitcomposition. Irrig. Sci. 31, 333–341.

Bastiaansssen, W.G.M., Brito, R.A.L., Bos, M.G., Souza, R.A., Cavalcanti, E.B., Bakker, M. M., 2001. Low cost satellite data for monthly irrigation performance monitoring: benchmarks from Nilo Coelho, Brazil. Irrig. Drain. Syst. 15, 53–79.

Bastiaansssen, W.G.M., Menenti, M., Feddes, R.A., Roerink, G.J., Holtslag, A.A.M., 1998. A remote sensing surface energy balance algorithm for land (SEBAL) 1. Formulation. J. Hydrol. 212–213, 198–212.

Bhattarai, N., Quackenbush, L.J., Im, J., Shaw, S.B., 2017b. A new optimized algorithm for automating endmember pixel selection in the SEBAL and METRIC models. Remote Sens. Environ. 196, 178–192.

Bhattarai, N., Wagle, P., Gowda, P.H., Kakani, V.G., 2017a. Utility of remote sensing-based surface energy balance models to track water stress in rain-fed switchgrass under dry and wet conditions. ISPRS J. Photogramm. Remote Sens. 113, 128–141.

Bos, M.G., Burton, M.A., Molden, D.J., 2015. Irrigation and Drainage Performance Assessments. Practical Guidelines. CABI Publishing, Cambridge, USA.

Cabral, O.M.R., Rocha, H.R., Gash, J.H., Freitas, H.C., Ligo, M.A.V., 2015. Water and energy fluxes from a woodland savanna (cerrado) in southeast Brazil. J. Hydrol. 4, 22–40.

Cancela, J.J., González, X.P., Vilanova, M., Mirás-Avalos, J.M., 2019. Water management using drones and satellites in Agriculture. Water 11, 874. https://doi.org/10.3390/w11050874.

Castelli, M., Asam, S. , Jacob, A. , Zebisch , M. , Notarnicola , C. , 2018. Monitoringdaily evapotranspiration in the Alps exploiting Sentinel-2 and meteorologicaldata. Proceedings of the Remote Sensing andHydrology Symposium (ICRS-IAHS), Cordoba, Spain, May 8-10, 2018.

Chai, Q., Gan, Y., Zhao, C., Xu, H.L., Waskom, R.M., Niu, Y., Siddique, K.H.M., 2016. Regulated deficit irrigation for crop production under drought stress. A review. Agron. Sustain. Dev. 36, 3.

Cleugh, H.A., Leuning, R., Mu, Q., Running, S.W., 2007. Regional evaporation estimates from flux tower and MODIS satellite data. Remote Sens. Environ. 106, 285–304.

Coaguila, D.N., Hernandez, F.B.T., Teixeira, A.H. de C., Franco, R.A.M., Leivas, J.F.L., 2017. Water productivity using SAFER - simple algorithm for evapotranspiration retrieving in watershed. Rev. Bras. Eng. Agr. Amb. 21, 524–529.

Consoli, S., Licciardello, F., Vanella, D., Pasotti, L., Villani, G., Tomei, F., 2016. Testing the water balance model CRITERIA using TDR measurements, micrometeorological data and satellite-based information. Agric. Water Manag. 170, 68–80.

Consoli, S., O'Connell, N., Snyder, R., 2006. Estimation of evapotranspiration of different sized navel-orange tree orchards using energy balance. J. Irrig. Drain. Eng. 132, 2–8.

Consoli, S., Papa, R., 2013. Corrected surface energy balance to measure and model the evapotranspiration of irrigated orange orchards in semi-arid Mediterranean conditions. Irrig. Sci. 31, 1159–1171.

Consoli, S., Stagno, F., Vanella, D., Boaga, J., Cassiani, G., Roccuzzo, G., 2017. Partial root-zone drying irrigation in orange orchards: effects on water use and crop production characteristics. Eur. J. Agron. 82, 190–202.

Consoli, S., Vanella, D., 2014. Comparisons of satellite-based models for estimating evapotranspiration fluxes. J. Hydrol. 513, 475–489.

Costa , D.S.M. , Ruas , K.F. , Pereira , A.M. , 2010. Aspotencialidades da região semiárida do Norte de Minas Gerais: Análise do Centrode Estudos de Convivência com o Semiárido. Anais do XVI EncontroNacional dos Geógrafos, Porto Alegre, Brasil, 2010;AGB: Lavras-MG, Brasil, p. 1–10.

Dahan, O., Babad, A., Lazarovitch, N., Russak, E.E., Kurtzman, D., 2014. Nitrate leaching from intensive organic farms to groundwater. Hydrol. Earth Syst. Sci. 18, 333–341.

Fandiño, M., Cancela, J.J., Rey, B.J., Martínez, E.M., Rosa, R.G., Pereira, L.S., 2012. Using the dual-K_c approach to model evapotranspiration of Albariño vineyards (*Vitis vinifera* L. cv. Albariño) with consideration of active ground cover. Agric. Water Manag. 112, 75–87.

Fernández, J.E., Alcon, F., Diaz-Espejo, A., Hernandez-Santana, V., Cuevas, M.V., 2019. Water productivity and economic analyses for super high-density olive orchards. Acta Hortic.
García Tejero, I.F., Durán Zuazo, V.H., Rubio Casal, A.E., 2019. Deficit-irrigation strategies to enhance the water productivity in orange trees in semi-arid environments. J. Agric. Food Dev. 5, 43–51.
García-Tejero, I.F., Durán-Zuazo, V.H., Muriel-Fernández, J.L., Jiménez-Bocanegra, J.A., 2011. Linking canopy temperature and trunk diameter fluctuations with other physiological water status tools for water stress management in citrus orchards. Funct. Plant Biol. 38, 106–117.
Garcia-Tejero, I.F., Romero-Vicente, R., Jiménez-Bocanegra, J.A., Martínez-García, G., Durán-Zuazo, V.H., Muriel-Fernández, J.L., 2010. Response of citrus trees to deficit irrigation during different phenological periods in relation to yield, fruit quality, and water productivity. Agric. Water Manag. 97, 689–699.
Germaná, C., Sardo, V., 2004. Determination when to initiate irrigation of orange trees. Acta Hortic. 664, 591–597.
Gonçalves, A.B.S., Azevedo, C.D.V., Oliveira, M.T., Romualdo, M.A.F., Fernandes, M.R. F., 2020. Perfil da Fruticultura 2020: Base de dados de 2018 e 2019. SEAPA - Secretaria de Estado de Agricultura. Pecuária e Abastecimento, Belo Horizonte-MG, Brazil.
Gong, X., Liu, H., Sun, J., Gao, Y., Zhang, H., 2019. Comparison of Shuttleworth-Wallace model and dual crop coefficient method for estimating evapotranspiration of tomato cultivated in a solar greenhouse. Agric. Water Manag. 217, 141–153.
González-Altozano, P., Castel, J.R., 1999. Regulated deficit irrigation in 'Clementina de Nules' citrus trees. I: yield and fruit quality effects. J. Hortic. Sci. Biotechnol. 74 (6), 706–713.
Gu, Z., Qi, Z., Ma, L., Gui, D., Xu, J., Fang, Q., Yuan, S., Feng, G., 2017. Development of an irrigation scheduling software based on model predicted crop water stress. Comput. Electron. Agric. 143, 208–221.
Hatfield, J.L., Dold, C., 2019. Water-use efficiency: advances and challenges in a changing climate. Front. Plant Sci. 10, 103.
Holtzman, M.E., Carmona, F., Rivas, R., Niclòs, R., 2018. Early assessment of crop yield from remotely sensed water stress and solar radiation data. ISPRS J. Photogramm. Remote Sens. 145, 297–306.
Hutton, R.J., Loveys, B.R., 2011. A partial root zone drying irrigation strategy forcitrus – effects on water use efficiency and fruit characteristics. Agric. Water Manag. 98, 1485–1496.
Jaafar, H.H., Amad, F.A., 2020. Time series trends of Landsat-based ET using automated calibration in METRIC and SEBAL: the Bekaa Valley, Lebanon. Remote Sens. Environ. 238, 111034.
Jamshidi, S., Zand-Parsa, S., Kamgar-Haghighi, A.A., Shahsavar, A.R., Niyogi, D., 2020. Evapotranspiration, crop coefficients, and physiological responses of citrus trees in semi-arid climatic conditions. Agric. Water Manag. 227, 105838.
Junior, C.R.A.B., Folegatti, M.V., Rocha, F.J., Atarassi, R.T., 2008. Coeficiente de cultura da lima-ácida Tahiti no outono-inverno determinado por lisimetria de pesagem em Piracicaba-SP. Eng. Agr. 28, 691–698.
Kamble, B., Kilic, A., Hubard, K., 2013. Estimating crop coefficients using remote sensing-based vegetation index. Remote Sens. 5, 1588–1602.
Lee, Y., Kim, S., 2016. The modified SEBAL for mapping daily spatial evapotranspiration of South Korea using three flux towers and Terra MODIS data. Remote Sens. 8, 983.
Leivas, J.F., Teixeira, A.H. de C., Bayma-Silva, G., Ronquim, C.C., Reis, J.B.R.S., 2016. Biophysical indicators based on satellite images in an irrigated area at the São Francisco River basin. Proc. SPIE 9998, 99981N-1–99981N-9.
Longo-Minnolo, G., Vanella, D., Consoli, S., Intrigliolo, D.S., Ramirez-Cuesta, J.M., 2020. Integrating forecast meteorological data into the ArcDualKc model for estimating spatially distributed evapotranspiration rates of a citrus orchard. Agric. Water Manag. 231, 105967.
Lumbreras , J.F. , Naime , U.J. , Oliveira , A.P. de , SilvaNeto , L. de F. da , Carvalho Filho , A. de, Motta , P.E.F. da, Calderano, S.B., Simões, M.L.R. , Aglio , M.L.D. , Vieira , E. M. , Machado , M.L., Santos, A.J.R. dos , Silva, D.C. da, Souza , J.S. de, Ferreira , A. R., 2014. Levantamento semi detalhado dos solos do Projeto Jaíba(Etapa III), Estado de Minas Gerais; Embrapa Solos: Rio de Janeiro, Brasil.
Lu, N., Chen, S., Wilske, B., Sun, G., Chen, J., 2011. Evapotranspiration and soil water relationships in a range of disturbed and undisturbed ecosystems in the semi-arid Inner Mongolia, China. J. Plant Ecol. 4, 49–60.
Maestre-Valero, J., Testi, L., Jiménez-Bello, M., Castel, J.R., Intrigliolo, D.S., 2017. Evapotranspiration and carbon exchange in a citrus orchard using eddy covariance. Irrig. Sci. 35, 397–408.
Marin, F.R., Angelocci, L.R., Nassif, D.S.P., Vianna, M.S., Pilau, F.G., da Silva, E.H.M., Sobenko, L.R., Gonçalves, A.O., Pereira, R.A.A., Carvalho, K.S., 2019. Revisiting the crop coefficient–reference evapotranspiration procedure for improving irrigation management. Theor. Appl. Climatol. 138, 1785–1793. https://doi.org/10.1007/s00704-019-02940-7.
Mata-González, R., McLendon, T., Martin, D.W., 2005. The inappropriate use of crop transpiration coefficients (K_c) to estimate evapotranspiration in arid ecosystems: a review. Arid Land Res. Manag. 19, 285–295.
Mateos, L., González-Dugo, M.P., Testi, L., Villalobos, F.J., 2013. Monitoring evapotranspiration of irrigated crops using crop coefficients derived from time series of satellite images. I. Method validation. Agric. Water Manag. 125, 81–91.
Melgar, J.C., Dunlop, J.M., Syvertsen, J.P., 2010. Growth and physiological responses of the citrus rootstock Swingle citrumelo seedlings to partial rootzone drying and deficit irrigation. J. Agric. Sci. 148 (05), 593–602.
Mhawej, M., Caiserman, A., Nasrallah, A., Dawi, A., Bachour, R., Faour, G., 2020a. Automated evapotranspiration retrieval model with missing soil-related datasets: The proposal of SEBALI. Agric. Water Manag. 229, 105938.
Mhawej, M., Elias, G., Nasrallah, A., Faour, G., 2020b. Dynamic calibration for better SEBALI ET estimations: Validations and recommendations. Agric. Water Manag. 230, 105955.
Mokhtari, A., Noory, H., Pourshakouri, F., Haghighatmehr, P., Afrasiabian, Y., Razavi, M., Fereydooni, F., Naeni, A.S., 2019. Calculating potential evapotranspiration and single crop coefficient based on energy balance equation using Landsat 8 and Sentinel-2. ISPRS J. Photogram. Remote Sens. 154, 231–245.
Nagler, P.L., Glenn, E.P., Nguyen, U., Scott, R.L., Doody, T., 2013. Estimating riparian and agricultural actual evapotranspiration by reference evapotranspiration and MODIS enhanced vegetation index. Remote Sens. 5, 3849–3871.
Nawaz, R., Abbasi, N.A., Hafiz, I.A., Azeem Khalid, A., 2020. Impact of climate variables on growth and development of Kinnow fruit (*Citrus nobilis* Lour x *Citrus deliciosa* Tenora) grown at different ecological zones under climate change scenario. Sci. Hortic., 108868
Niziński, J.J., Ziernicka-Wojtaszek, A., Książek, L., Gawroński, K., Montoroi, J.-P., Zaghloul, A., Ali, R.R., Saber, M., 2017. Actual evapotranspiration of the orange orchard in Northern Sinai. Egypt. Acta Sci. Pol. Form. Circumiectus 16 (4), 187–203.
Nyoley, D., Nsaali, M., Minaya, V., van Griensven, A., Mbilinyi, B., Diels, J., Hessels, T., Kahimba, F., 2019. High resolution mapping of agricultural water productivity using SEBAL in a cultivated African catchment, Tanzania. Phys. Chem. Earth 112, 36–49.
Olivera-Guerra, L., Merlin, O., Er-Raki, S., Khabba, S., Escorihuela, M.J., 2018. Estimating the water budget components of irrigated crops: combining the FAO-56 dual crop coefficient with surface temperature and vegetation index data. Agric. Water Manag. 208, 120–131.
Panigrahi, P., Srivastava, A.K., 2016. Effective management of irrigation water in citrus orchard under a water scarce hot sub-humid region. Sci. Agric. 210, 6–13.
Panigrahi, P., Srivastava, A.K., Huchche, A.D., 2012. Effects of drip irrigation regimes and basin irrigation on Nagpur mandarin agronomical and physiological performance. Agric. Water Manag. 104, 79–88.
Pedroso, F.K.J.V., Prudente, D.A., Bueno, A.C.R., Machado, E.C., Ribeiro, R.V., 2014. Drought tolerance in citrus trees is enhanced by rootstock dependent changes in root growth and carbohydrate availability. Environ. Exp. Bot. 101, 26–35.
Rallo, G., González-Altozano, P., Manzano-Juárez, J., Provenzano, G., 2017. Using field measurements and FAO-56 model to assess the eco-physiological response of citrus orchards under regulated deficit irrigation. Agric. Water Manag. 180, 136–147.
Ramírez-Cuesta, J.M., Allen, R.G., Zarco-Tejada, P.J., Kilic, A., Santos, C., Lorite, I.J., 2019b. Impact of the spatial resolution on the energy balance components on an open-canopy olive orchard. Int. J. Appl. Earth Obs. Geoinf. 74, 88–102.
Ramírez-Cuesta, J.M., Miras-Avalos, J., Rubio-Asensio, J., Intrigliolo, D., 2019a. A novel ArcGIS toolbox for estimating crop water demands by integrating the dual crop coefficient approach with multi-satellite imagery. Water 11 (1), 38.
Ramírez-Cuesta, J.M., Vanella, D., Consoli, S., Motisi, A., Minacapilli, M., 2018. A satellite stand-alone procedure for deriving net radiation by using SEVIRI and MODIS products. Int. J. Appl. Earth Obs. Geoinf. 73, 786–799.
Rampazo, N.A.M., Picoli, M.C.A., Teixeira, A.H. de C., Cavaliero, C.K.N., 2020. Water consumption modeling by coupling MODIS images and agrometeorological data for sugarcane crops. Sugar Tech. https://doi.org/10.1007/s12355-020-00919-7.
Rana, G., Katerji, N., de Lorenzi, F., 2005. Measurement and modelling of evapotranspiration of irrigated citrus orchard under Mediterranean conditions. Agric. For. Meteorol. 128, 199–209.
Robles, J.M., Botiá, P., Pérez-Pérez, J.G., 2017. Sour Orange rootstock increases water productivity in deficit irrigated 'Viena' lemon trees compared with Citrus macrophylla. Agric. Water Manag. 186, 98–107.
Roerink, G.J., Su, Z., Menenti, M., 2000. S-SEBI: a simple remote sensing algorithm to estimate the surface energy balance. Phys. Chem. Earth 25, 147–157.
Romero-Conde, A., Kusakabe, A., Melgar, J.C., 2014. Physiological responses of citrus to partial rootzone drying irrigation strategies. Sci. Hortic. 169, 234–238.
Rosa, R.D., Ramos, T.B., Pereira, L.S., 2016. The dual K_c approach to assess maize and sweet sorghum transpiration and soil evaporation under saline conditions: application of the SIMDualKc model. Agric. Water Manag. 177, 77–94.
Rozenstein, O., Haymann, N., Kaplan, G., Tanny, J., 2018. Estimating cotton water consumption using a time series of Sentinel-2 imagery. Agric. Water Manag. 207, 44–52.
Sakthivadivel, R., de Fraiture, C., Molden, D.J., Perry, C., Kloezen, W., 1999. Indicators of land and water productivity irrigated agriculture. Int. J. Water Resour. Dev. 15, 161–180.
Santos, J.E.O., Cunha, F.F., Filgueiras, R., Silva, G.H., Teixeira, A.H. de C., Silva, F.C.S., Sediyama, G.C., 2020. Performance of SAFER evapotranspiration using missing meteorological data. Agric. Water Manag. 233, 1–8.
Silva, C.O.F., Manzione, R.L., Filho, J.L.A., 2018. Large-Scale spatial modeling of crop coefficient and biomass production in agroecosystems in southeast Brazil. Horticuturae 4, 1–20.
Silva, C.O.F., Teixeira, A.H. de C., Manzione, R.L., 2019. Agriwater: An R package for spatial modelling of energy balance and actual evapotranspiration using satellite images and agrometeorological data. Environ. Model. Softw. 120, 1–19.
Su, Z., 2002. The Surface Energy Balance System (SEBS) for estimation of turbulent heat fluxes. Hydrol. Earth Syst. Sci. 6, 85–99.
Tazekrit, I., Benslimane, M., Simonneaux, V., Hartani, T., Hamimed, A., 2018. Estimation of irrigation water pumping by remote sensing: application of the SAMIR model to citrus under mediterranean climate conditions. Rev. Bras. Meteorol. 33, 391–400.
Teixeira, A.H. de C., 2010. Determining regional actual evapotranspiration of irrigated and natural vegetation in the São Francisco river basin (Brazil) using remote sensing and Penman-Monteith equation. Remote Sens. 2, 1287–1319.
Teixeira, A.H. de C., Bastiaanssen, W.G.M., Ahmad, M.–ud–D., Bos, M.G., 2009a. Reviewing SEBAL input parameters for assessing evapotranspiration and water

productivity for the Low-Middle São Francisco River basin, Brazil Part B: calibration and validation. Agric. For. Meteorol. 149, 462–476.
Teixeira, A.H. de C., Bastiaanssen, W.G.M., Ahmad, M.–ud–D., Bos, M.G., 2009b. Reviewing SEBAL input parameters for assessing evapotranspiration and water productivity for the Low-Middle São Francisco River basin, Brazil Part B: application to the large scale. Agric. For. Meteorol. 149, 477–490.
Teixeira, A.H. de C., Bastiaanssen, W.G.M., Moura, M.S.B., Soares, J.M., Ahmad, M.–ud–D., Bos, M.G., 2008a. Energy and water balance measurements for water productivity analysis in irrigated mango trees, Northeast Brazil. Agric. For. Meteorol. 148, 1524–1537.
Teixeira, A.H. de C., Bastiaanssen, W.G.M., Moura, M.S.B., Soares, J.M., Ahmad, M.–ud–D., Bos, M.G., 2008b. Energy and water balance measurements for water productivity analysis in irrigated mango trees, Northeast Brazil. Agr. For. Meteorol. 148, 1524–1537.
Teixeira, A.H. de C., Hernandez, F.B.T., Andrade, R.G., Leivas, J.F., Victoria, D., de, C., Bolfe, E.L., 2014a. Irrigation performance assessments for corn crop with Landsat images in the São Paulo state, Brazil. Water Res. Irrig. Manag. 3, 91–100.
Teixeira, A.H. de C., Hernandez, F.B.T., Lopes, H.L., Scherer-Warren, M., Bassoi, L.H., 2014b. A comparative study of techniques for modeling the spatiotemporal distribution of heat and moisture fluxes in different agroecosystems in Brazil. In: Petropoulos, G.P. (Ed.), Remote Sensing of Energy Fluxes and Soil Moisture Content, first ed., 2014. CRC Press, Taylor and Francis Group, Boca Raton, FL, USA, pp. 169–191.
Teixeira, A.H. de C., Leivas, J.F., Hernandez, F.B.T., Franco, R.A.M., 2017b. Large-scale radiation and energy balances with Landsat 8 images and agrometeorological data in the Brazilian semiarid region. J. Appl. Remote Sens. 11, 016030.
Teixeira, A.H. de C., Leivas, J.F., Ronquim, C.C., Bayma-Silva, G., 2017a. The use of MODIS images to quantify the energy balance in different agroecosystems in Brazil. In: Rustamov, R.B., Hasanova, S., Zeynalova, M.H. (Eds.), Multi-Purposeful Application of Geospatial Data. Intech Open Limited, London, EC3R 6AF, UK, pp. 105–121.
Teixeira, A.H. de C., Leivas, J.F., Simão, F.R., Reis, J.B.R.S., 2018. Remote sensing drought indices for the semi-arid region of Southeast Brazil. Mod. Environ. Sci. Eng. 4, 537–545.
Teixeira, A.H. de C., Takemura, C.M., Leivas, J.F., Pacheco, E.P., Bayma-Silva, G., Garçon, E.A.M., 2019. Water productivity assessments for dwarf coconut by using Landsat 8 images and agrometeorological data. ISPRS J. Photogramm. Remote Sens. 155, 150–158.
Teixeira, A.H. de C., Takemura, C.M., Leivas, J.F., Pacheco, E.P., Silva, G.B., Garçon, E.A. M., 2020. Water productivity monitoring by using geotechnological tools in contrasting social and environmental conditions: applications in the São Francisco River basin, Brazil. Remote Sens. Appl. Soc. Environ. 18, 100296.
Vanella, D., Ramírez-Cuesta, J.M., Intrigliolo, D.S., Consoli, S., 2019. Combining electrical resistivity tomography and satellite images for improving evapotranspiration estimates of Citrus orchards. Remote Sens. 11 (4), 373.
Vanhellemont, Q., Ruddick, K., 2014. Turbid wakes associated with offshore wind turbines observed with Landsat 8. Remote Sens. Environ. 145, 105–115.
Vanino, S., Nino, P., Micheleb, C.D., Bolognesi, S.F., D'Urso, G., Bene, C.D., Pennelli, B., Vuolo, F., Farina, R., Pulighe, G., Napoli, R., 2018. Capability of Sentinel-2 data for estimating maximum evapotranspiration and irrigation requirements for tomato crop in Central Italy. Remote Sens. Environ. 215, 452–470.
Venancio, L.P., Mantovani, E.C., Amaral, C.H. do, Neale, C.M.U., Filgueiras, R., Ivo Zution Gonçalves, I.Z., Cunha, F.F. da, 2021. Evapotranspiration mapping of commercial corn fields in Brazil using SAFER algorithm. Sci. Agric. 78, 1–12.
Villalobos, F.J., Testi, L., Moreno-Perez, M.F., 2009. Evaporation and canopy conductance of citrus orchards. Agric. Water Manag. 96, 565–573.
Villalobos, F.J., Testi, L., Orgaz, F., García-Tejera, O., Lopez-Bernal, A., González-Dugo, M.V., Ballester-Lurbe, C., Castel, J.R., Alarcón-Cabañero, J.J., Nicolás-Nicolás, E., 2013. Modelling canopy conductance and transpiration of fruit trees in Mediterranean areas: a simplified approach. Agric. For. Meteorol. 171, 93–103.
Wagle, P., Kakani, V.G., Huhnke, R.L., 2016. Evapotranspiration and ecosystem water use efficiency of switchgrass and high biomass sorghum. Agron. J. 108, 1007–1019.
Wu, Bing-Fang, Xiong, Jun, Yan, Na-Na, Yang, Lei-Dong, Xin, Du, 2008. ETWatch for monitoring regional evapotranspiration with remote sensing. Adv. Water Sci. 19 (5), 671–678.
Yang, L.S., Yano, T.M.A., Li, S., 2003. Evapotranspiration of orange trees in greenhouse lysimeters. Irrig. Sci. 21, 145–149.
Zheng, C., Wang, Q., Li, P., 2016. Coupling SEBAL with a new radiation module and MODIS products for better estimation of evapotranspiration. Hydrol. Sci. J. 61 (8), 1535–1547.
Zhou, L., Zhou, G., 2009. Measurement and modeling of evapotranspiration over a reed (Phragmitesaustralis) marsh in Northeast China. J. Hydrol. 372, 41–47.
Zitouna-Chebbi, R., Mahjoub, I., Mekki, I., Ben Mechlia, N., 2015. Comparing evapotranspiration rates estimated from atmospheric flux, soil water balance and FAO56 method in a small orange orchard in Tunisia. In: VIII International Symposium on Irrigation of Horticultural Crops, 1150, pp. 23–30.